



Visible light emission from single walled carbon nanotube-noble metal nanoparticle composites

T. Pradeep

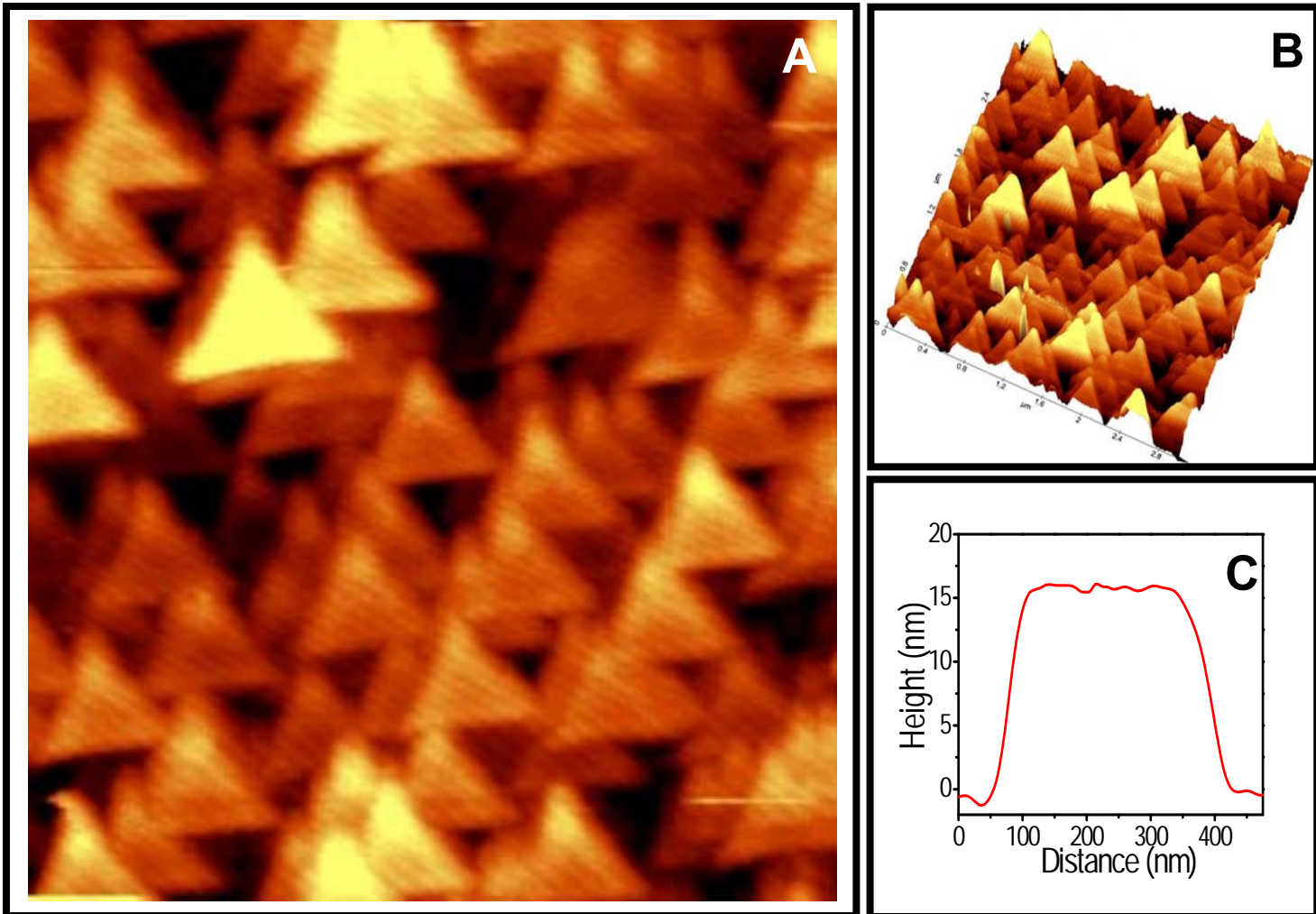
Department of Chemistry and Sophisticated Analytical Instrument Facility
Indian Institute of Technology Madras
Chennai 600 036

<http://www.dstuns.iitm.ac.in/pradeep-research-group.php>

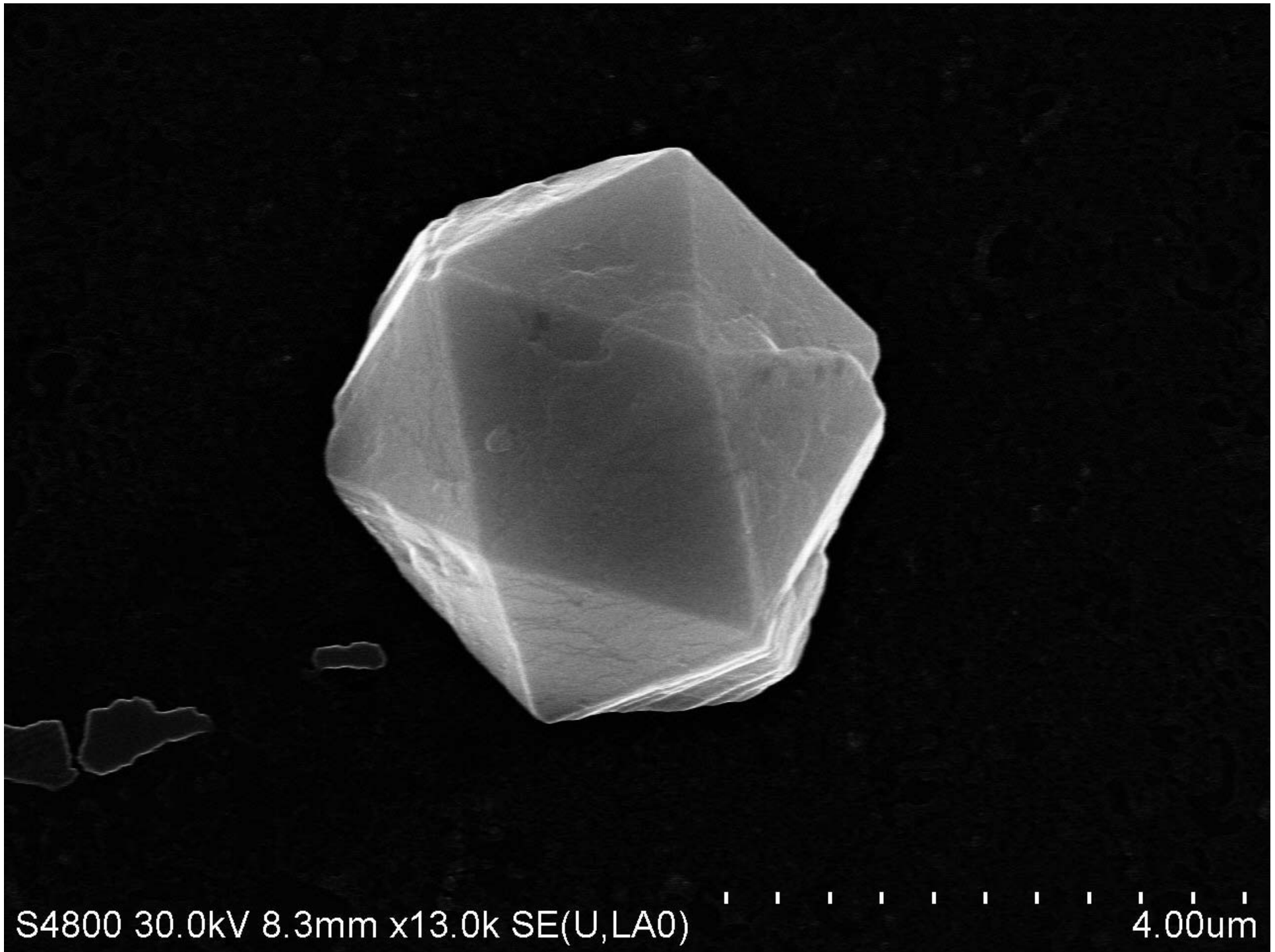


Acknowledgements
DST – Nanomission
Dr. C. Subramaniam
Dr. Jaydeb Chakrabarti
Prof. Takuji Ogawa
Mr. Chockalingam
Students

Chemical interactions with nanostructures leading to devices

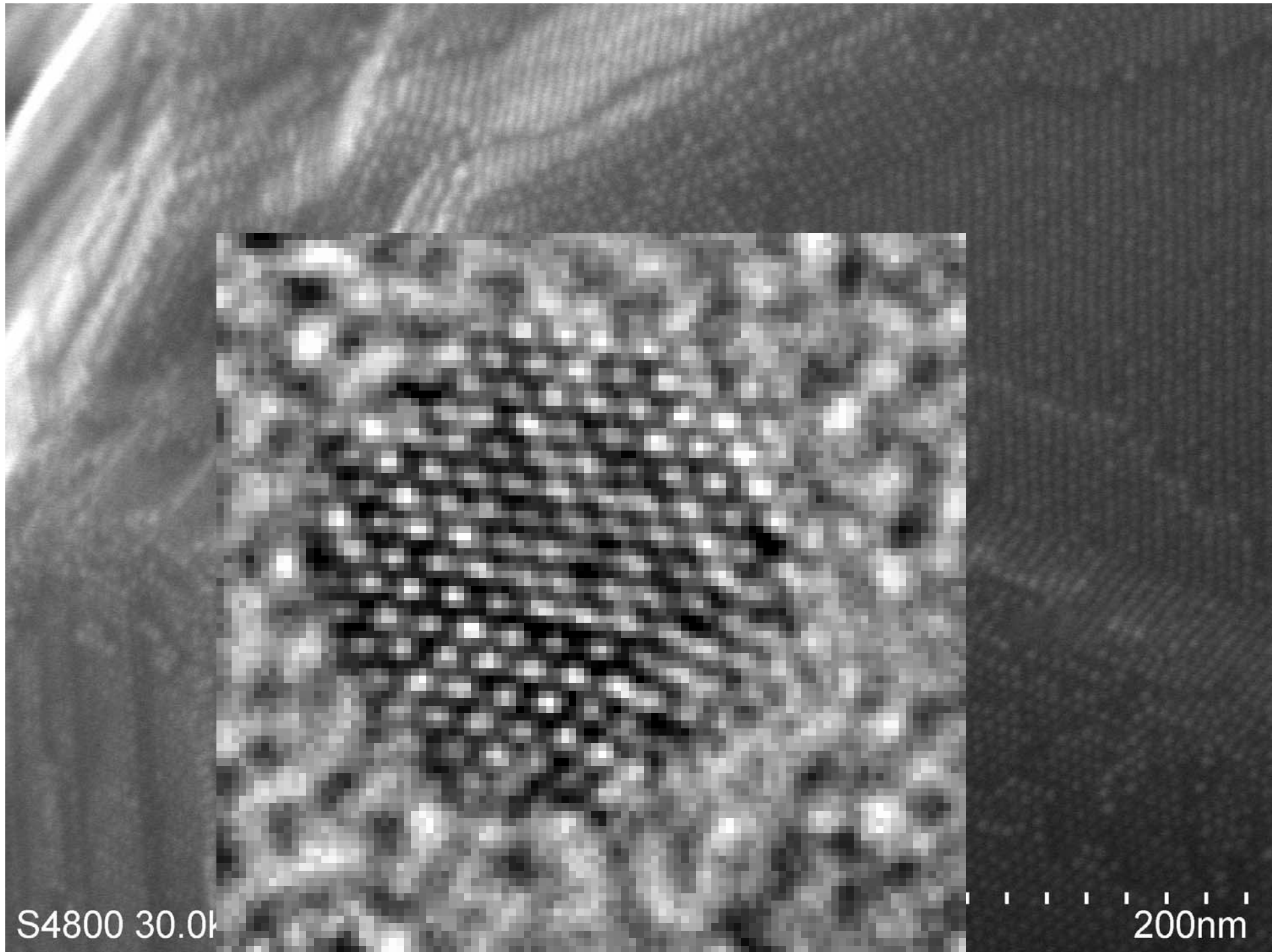


Sajanlal and Pradeep, Adv. Mater., 20 (2008) 980



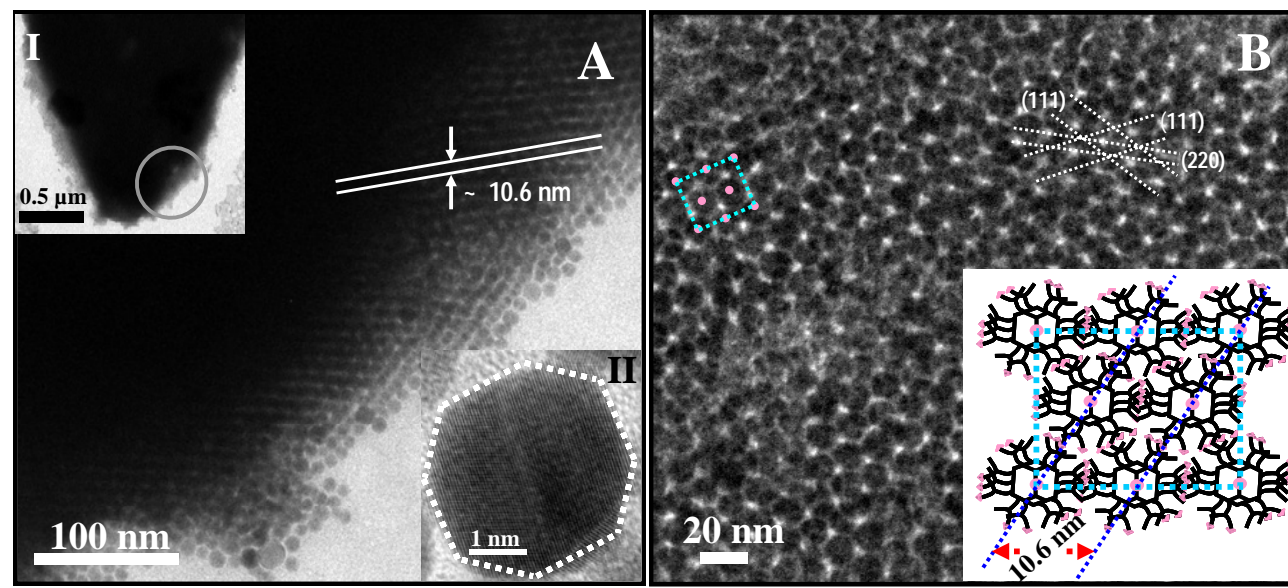
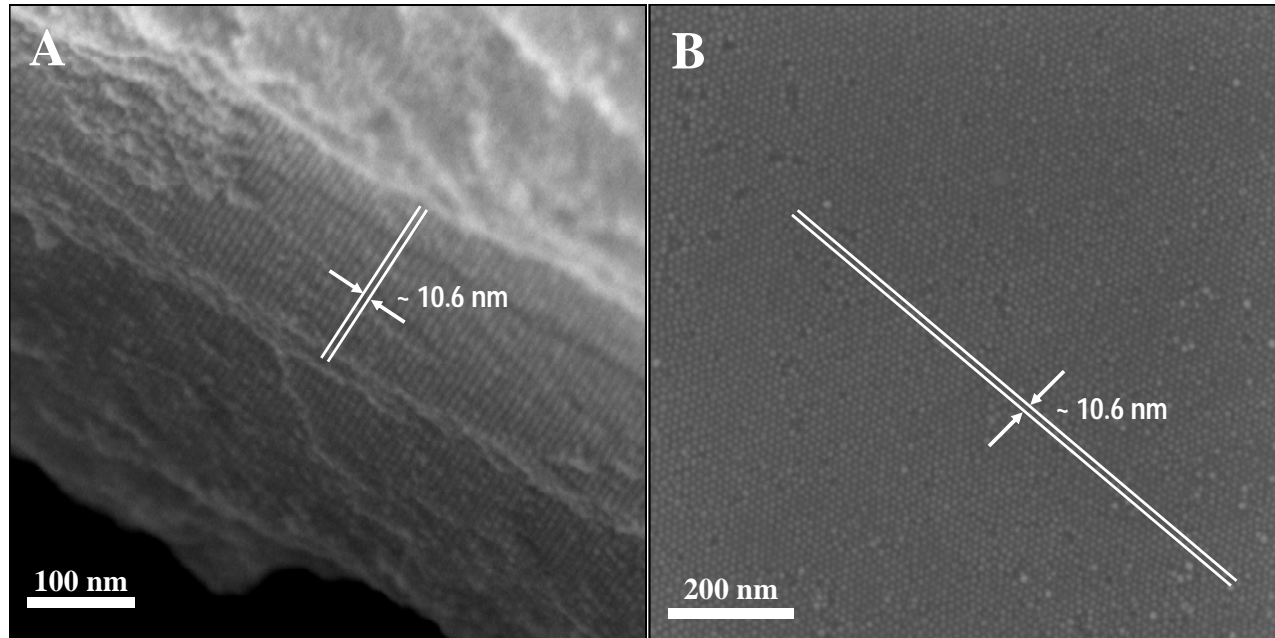
S4800 30.0kV 8.3mm x13.0k SE(U,LA0)

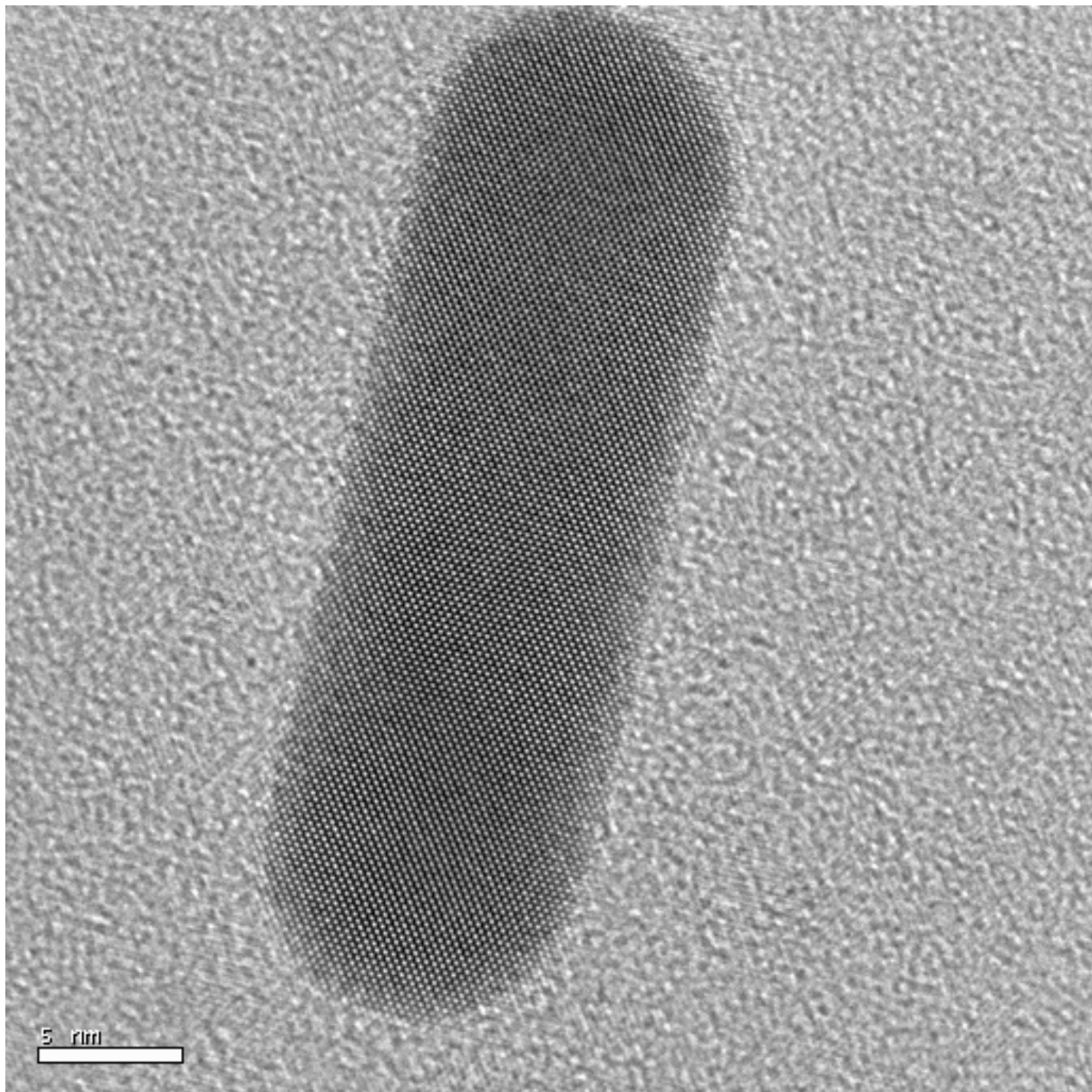
4.00um

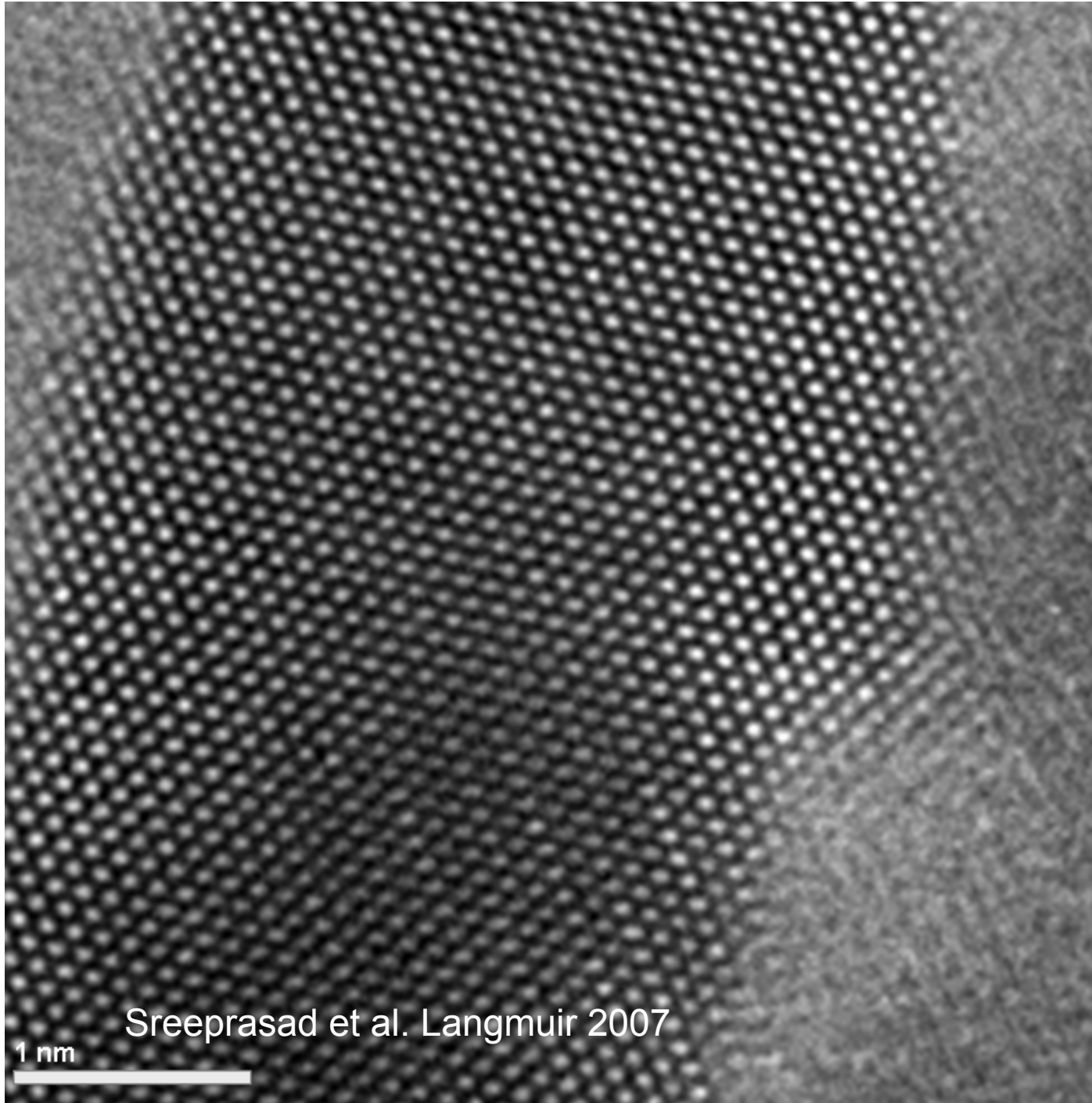


S4800 30.0k

200nm







Sreeprasad et al. Langmuir 2007

1 nm

In this talk.....

Visible emission from single walled carbon nanotubes

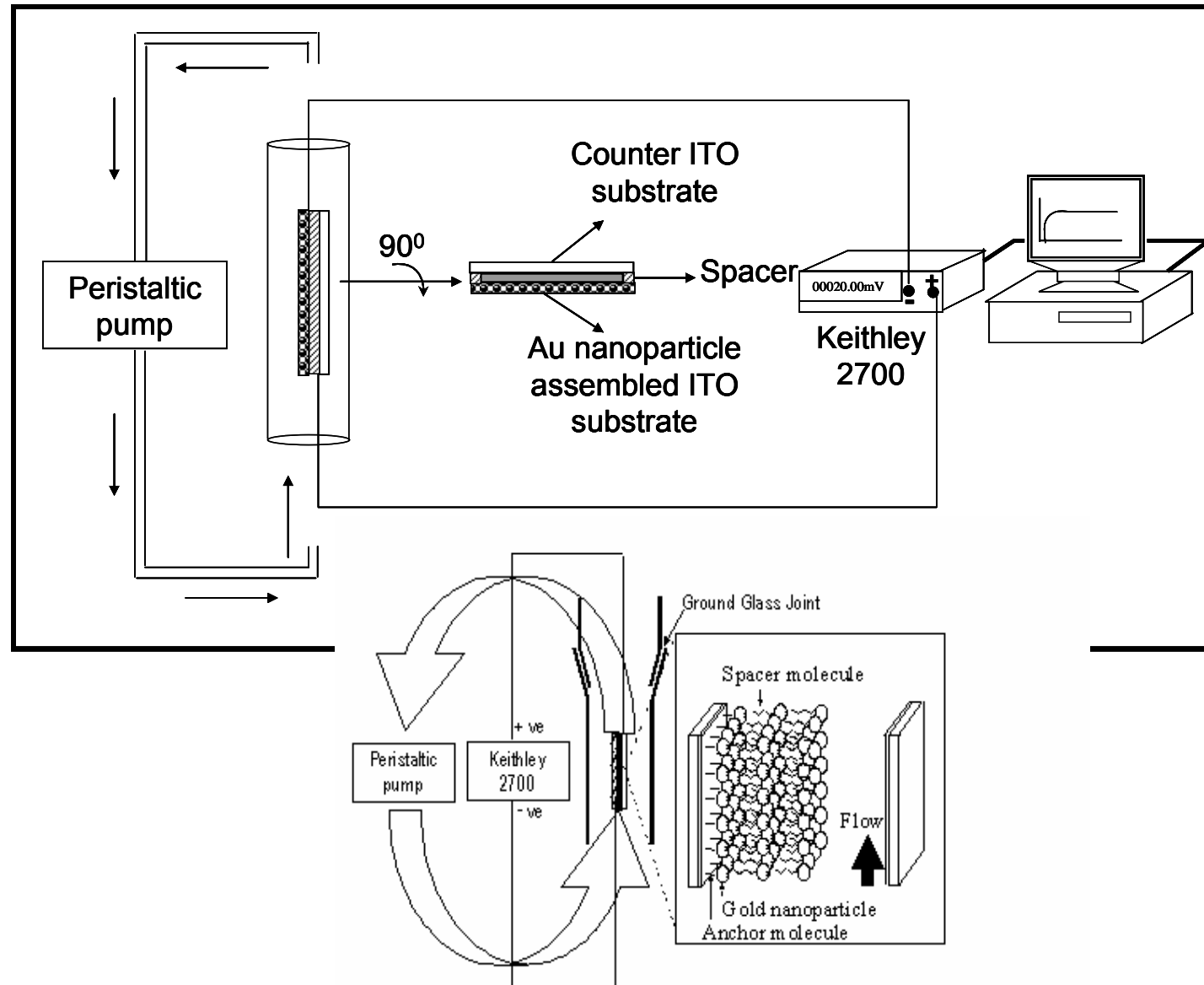
Background

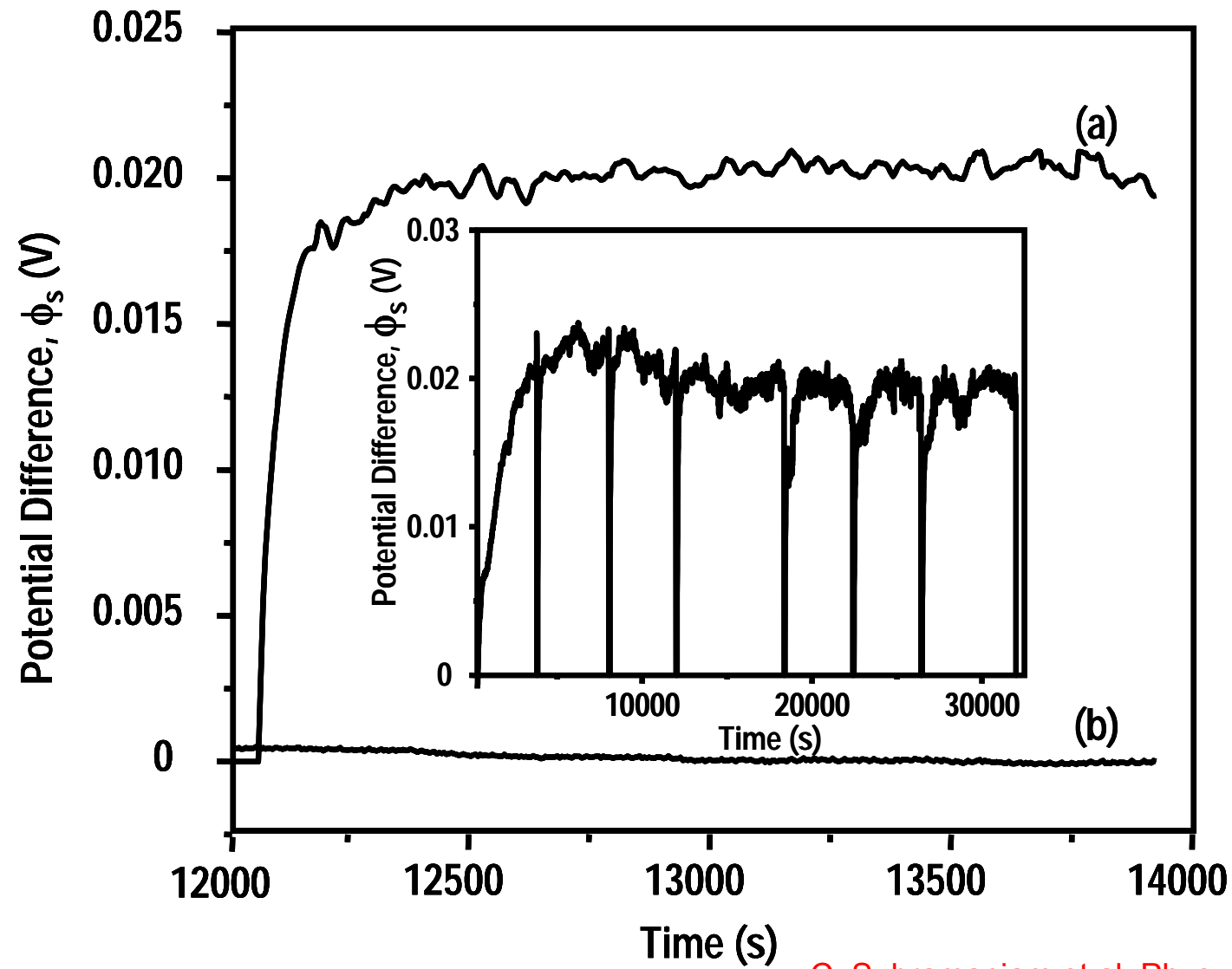
Experiment

Control experiments

Uses

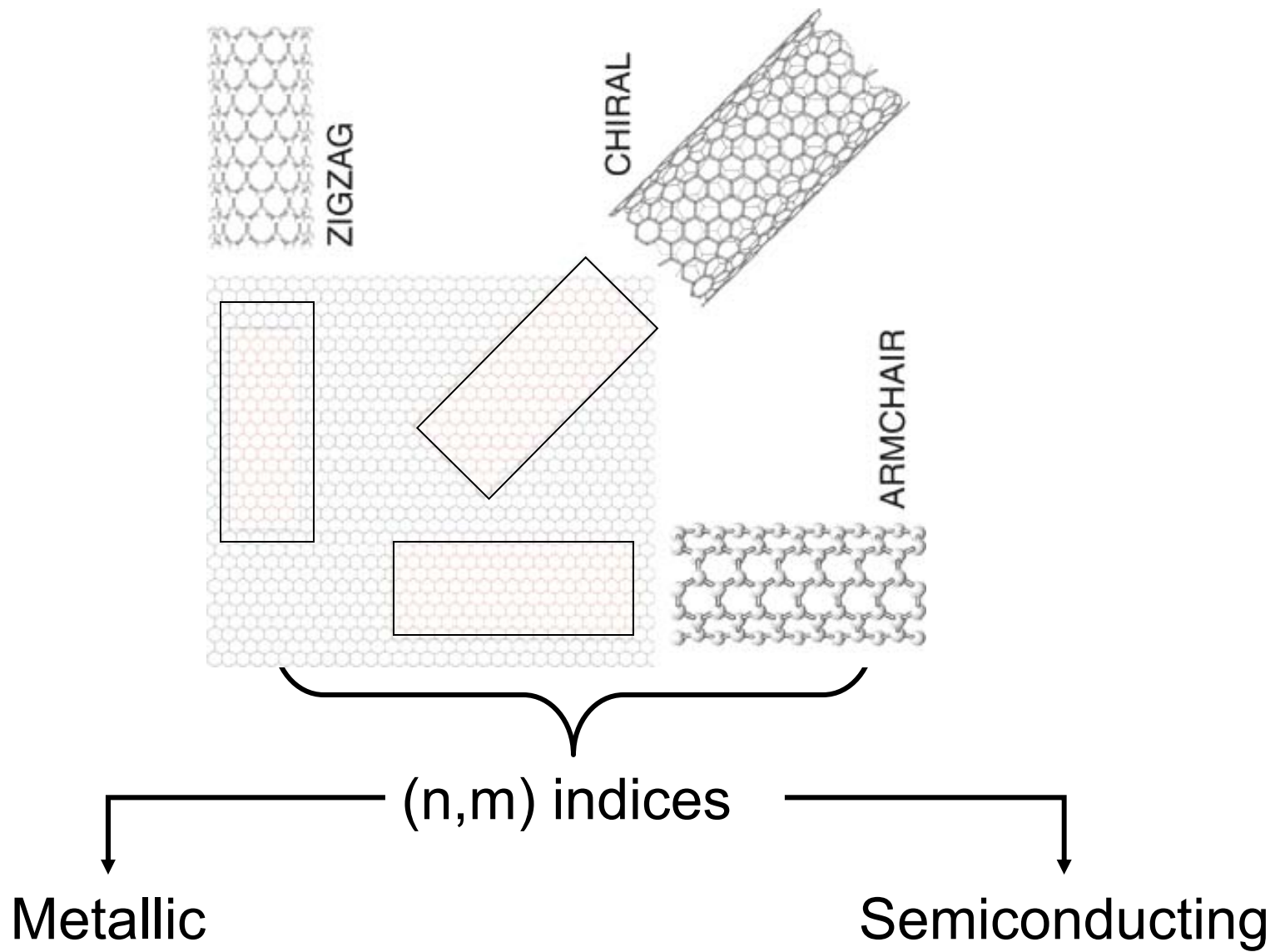
Flow induced potential in nanoparticle assemblies





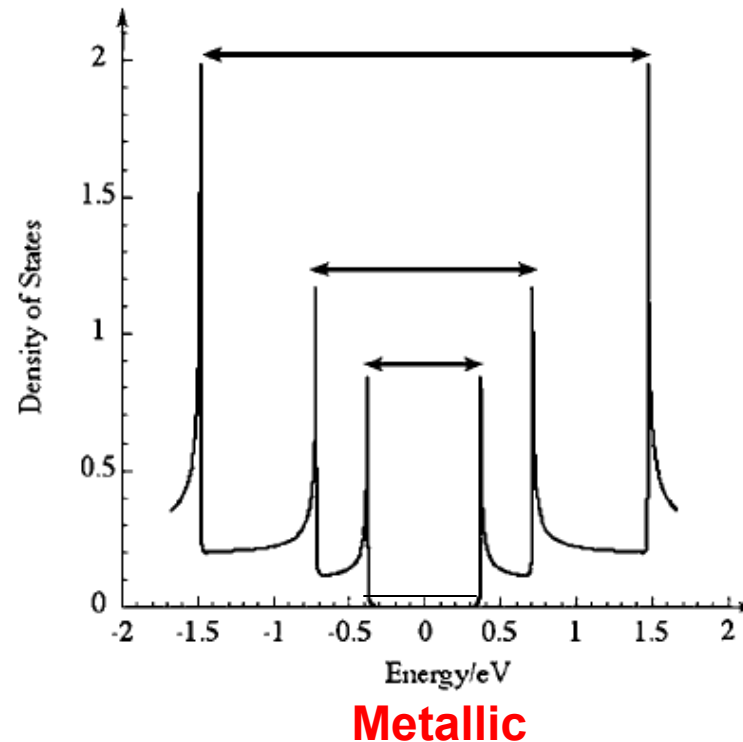
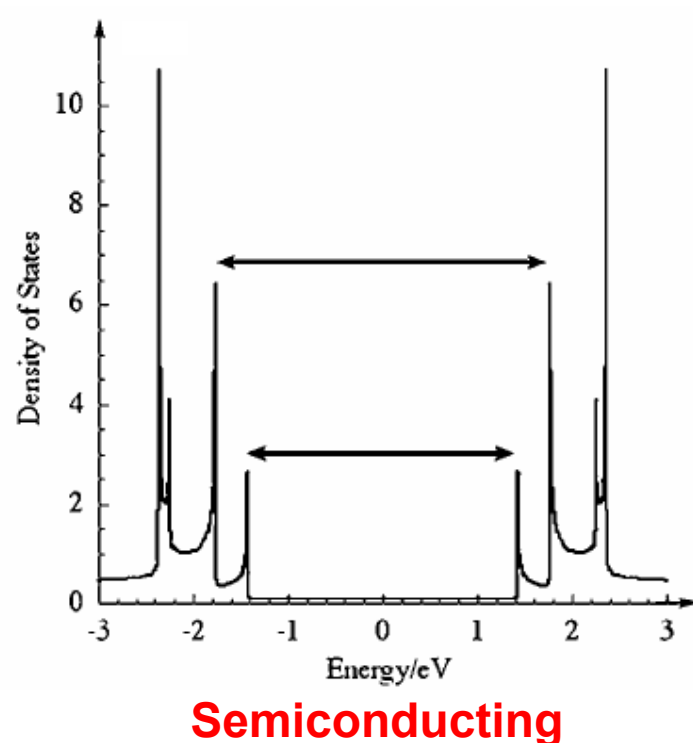
With Jaydeb Chakrabarti

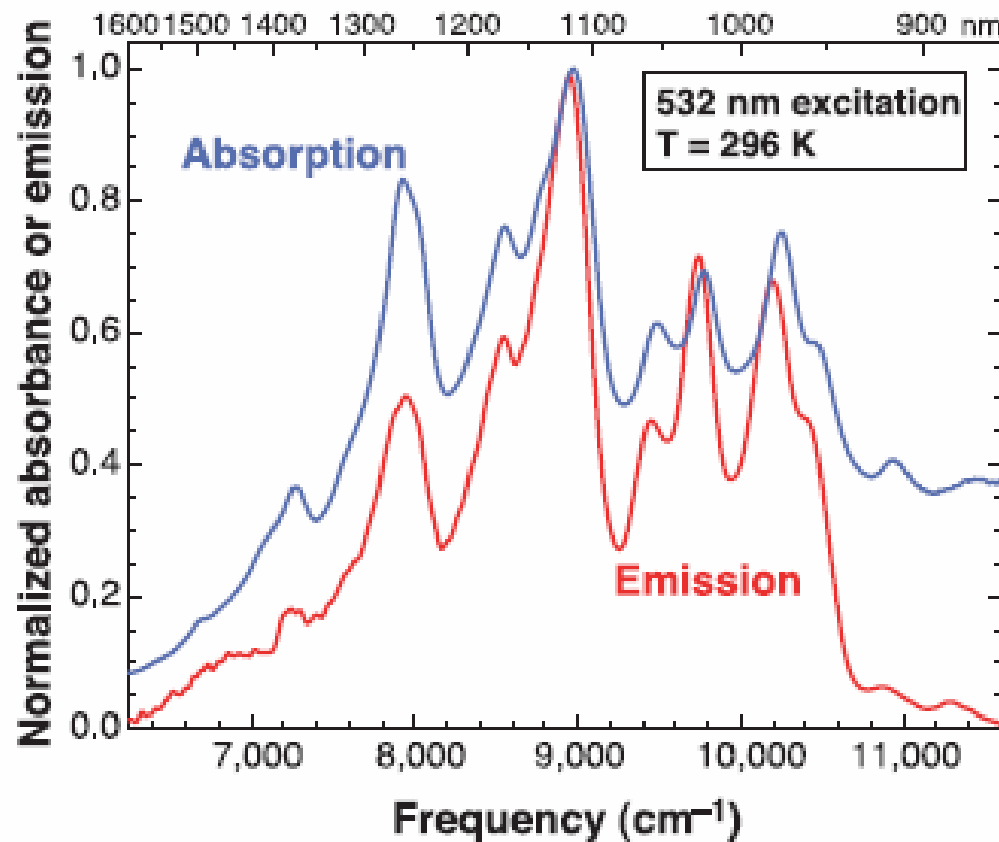
C. Subramaniam et al. Phys. Rev. Lett. 2005
J. Phys. Chem. C 2007
Indian Patent application 2005



Electrical transport properties

- Semiconducting : $(n-m) \neq 3l$. $E_g = 1.7 - 2.0 \text{ eV}$
- Metallic : $(n-m) = 3l$. $E_g = 0.0 - 0.5 \text{ eV}$





Emission spectrum (red) of individual fullerene nanotubes suspended in SDS micelles in D₂O excited by 8 ns, 532-nm laser pulses, overlaid with the absorption spectrum (blue) of the sample in this region of first van Hove band gap transitions.

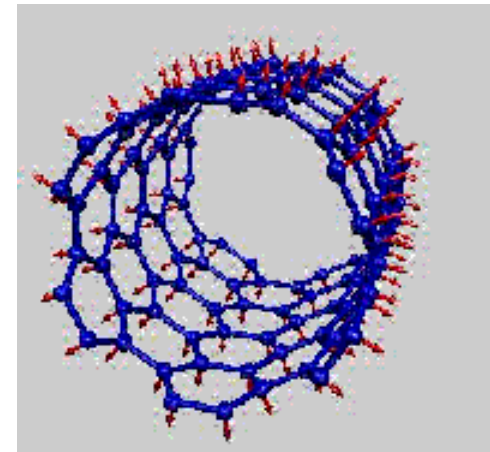
Sample is in liquid state.

M. J. O'Connell *et al.*, *Science* **297**, 593 (2002). 15

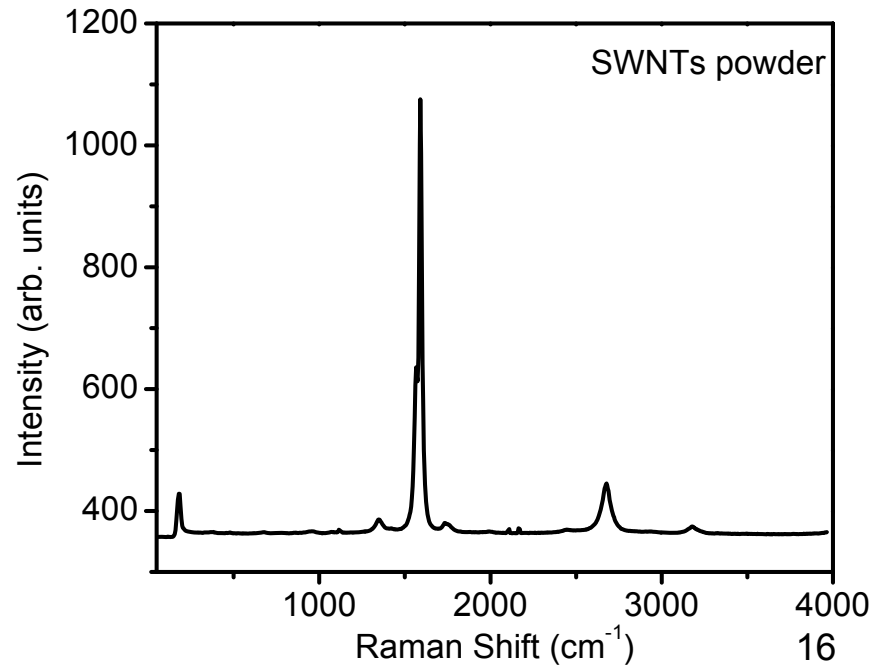
Raman spectroscopy of SWNTs

(A) Radial Breathing Mode (RBM)
Diameter dependent

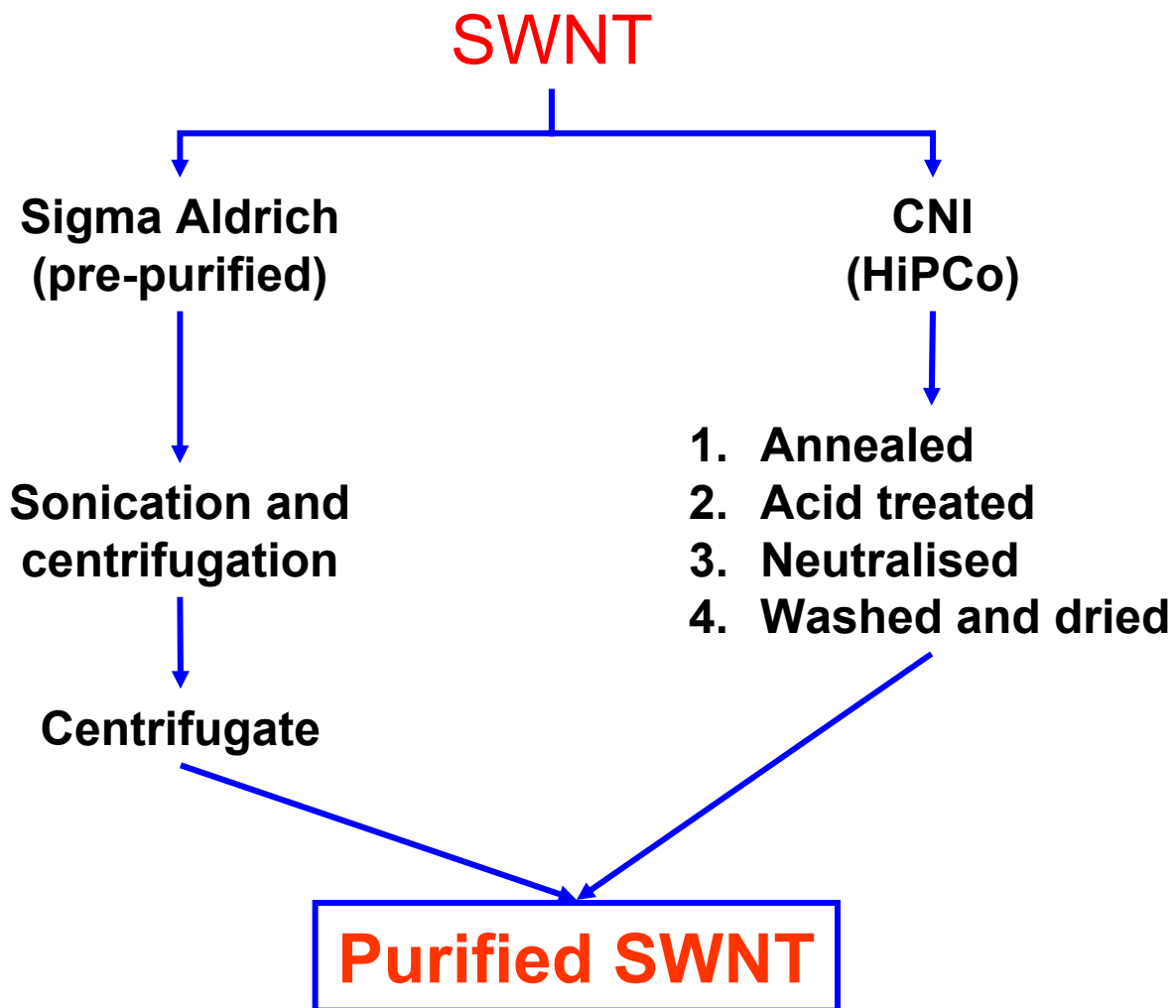
$$\omega_{RBM} (cm^{-1}) = \frac{224.8}{d_t (nm)} + 12.5$$



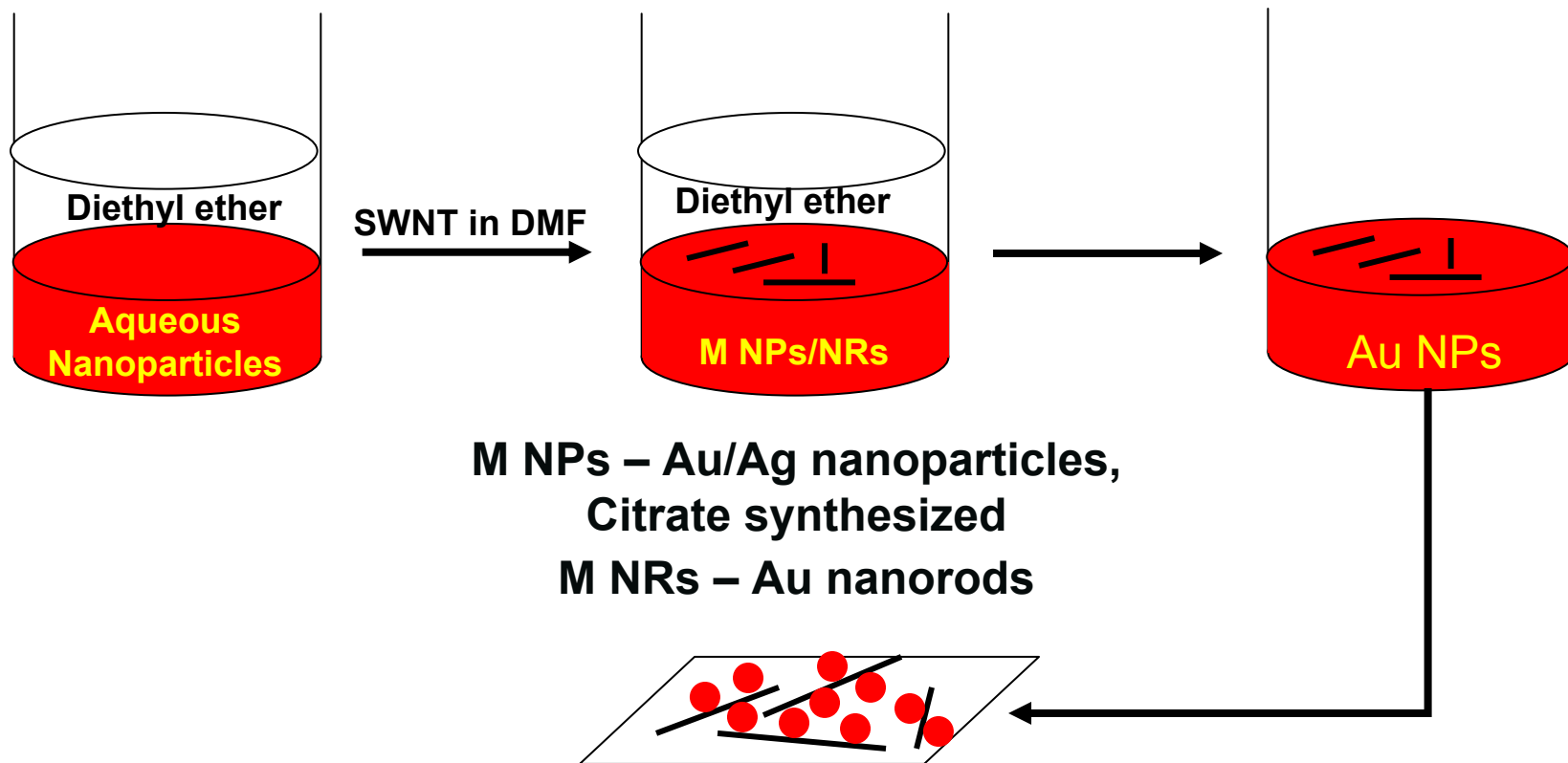
- (B) Tangential G band
In-plane vibrations
- (C) D-band
Defect centered
- (D) G` band
Occurs at $2\omega_D$



Purification of SWNT

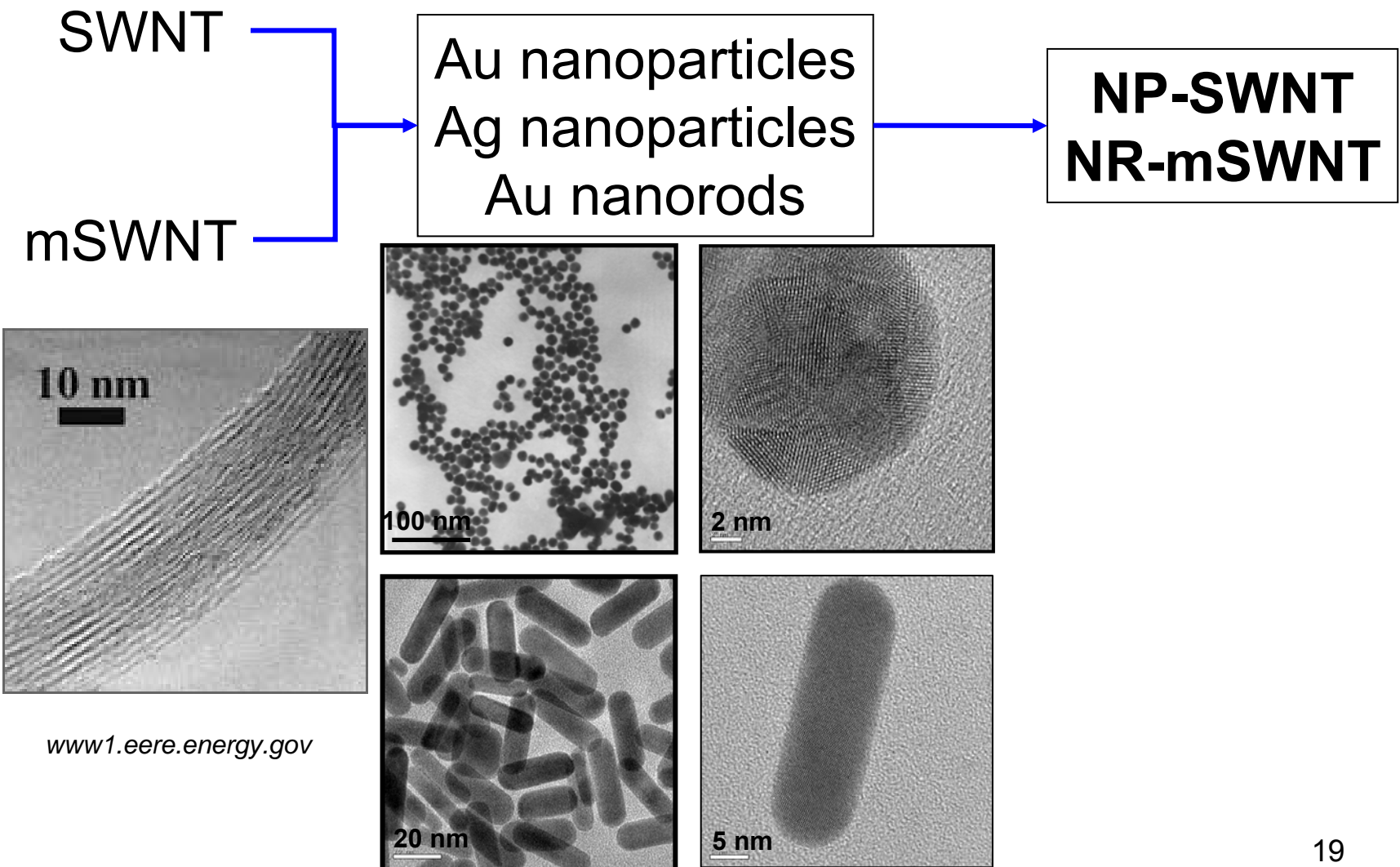


SWNT-nanoparticle composite

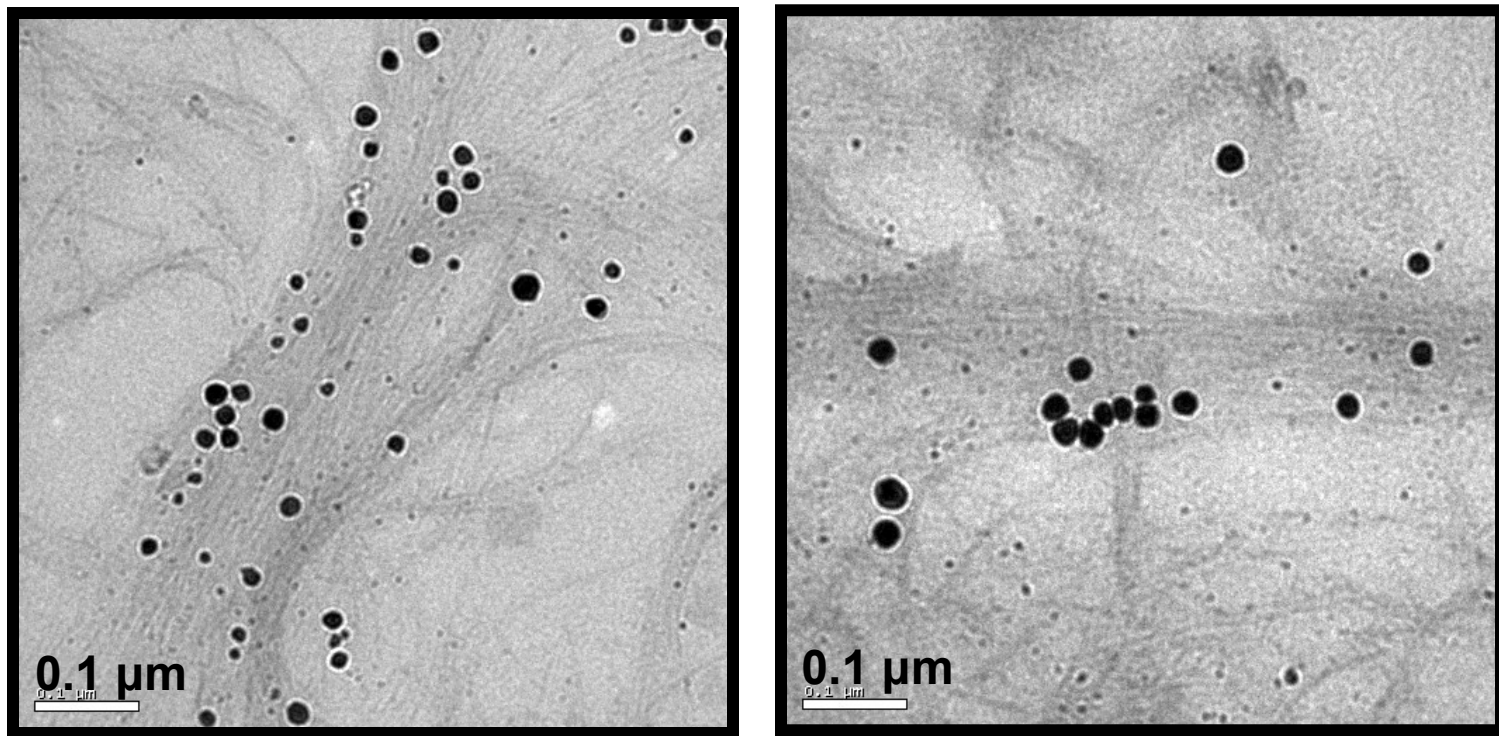


Sample is in solid state.

Starting materials

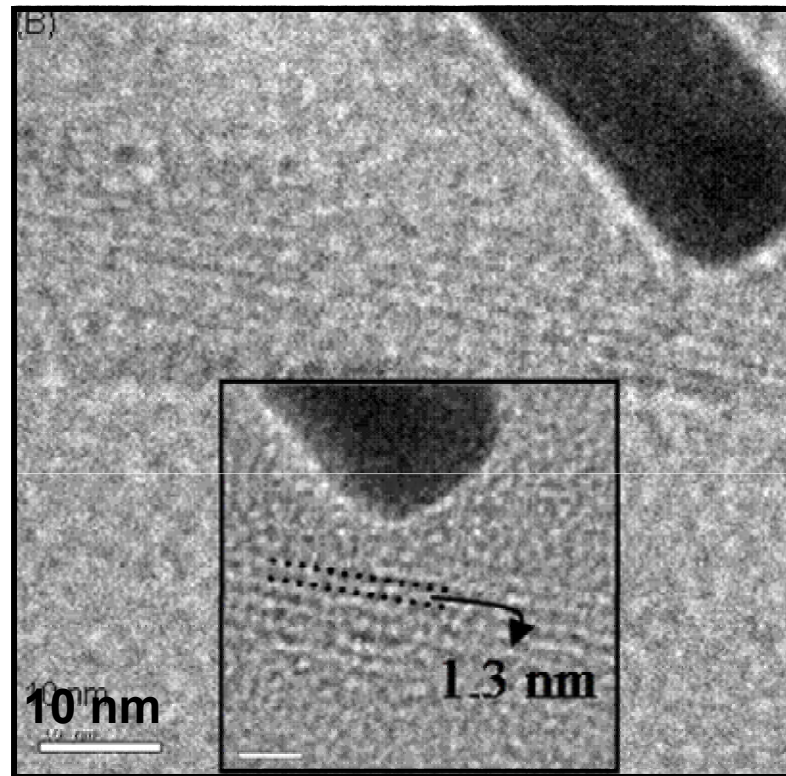


Nanoparticle composite



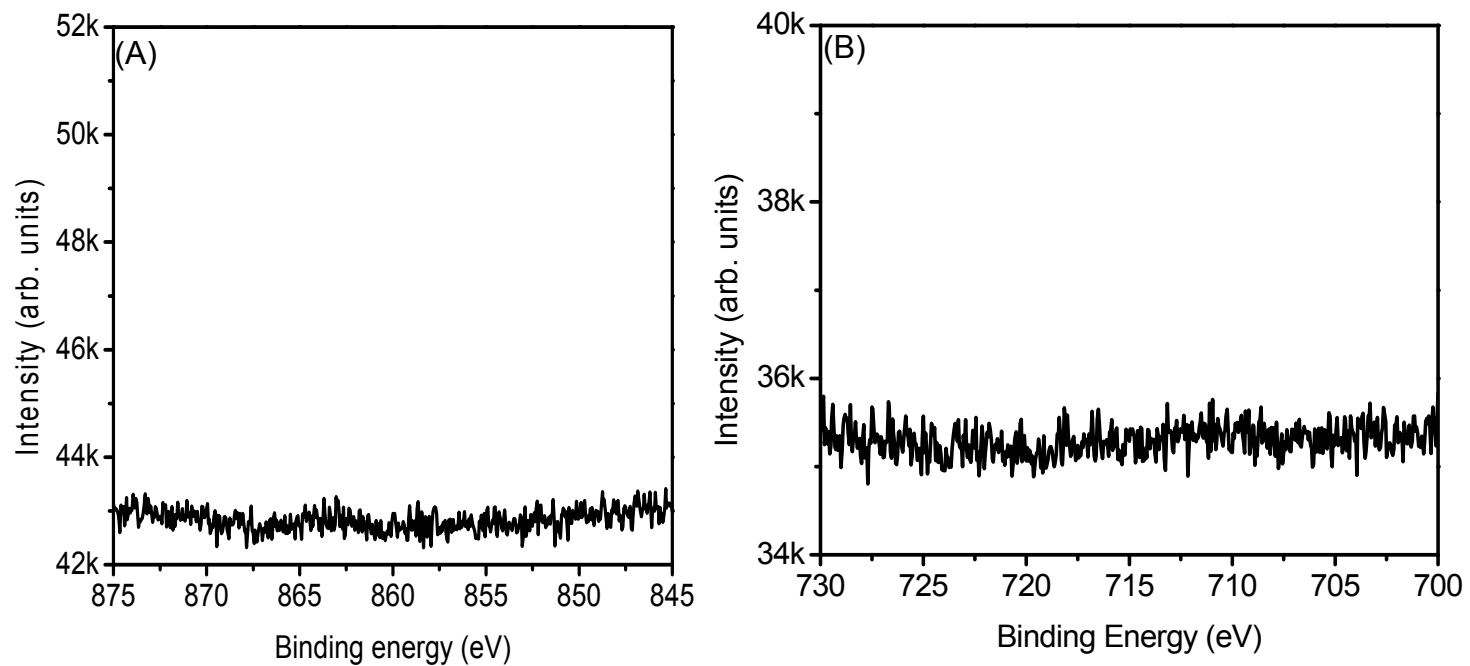
TEM images of Au-SWNTs composite acquired at 100 keV.

Nanorod composite

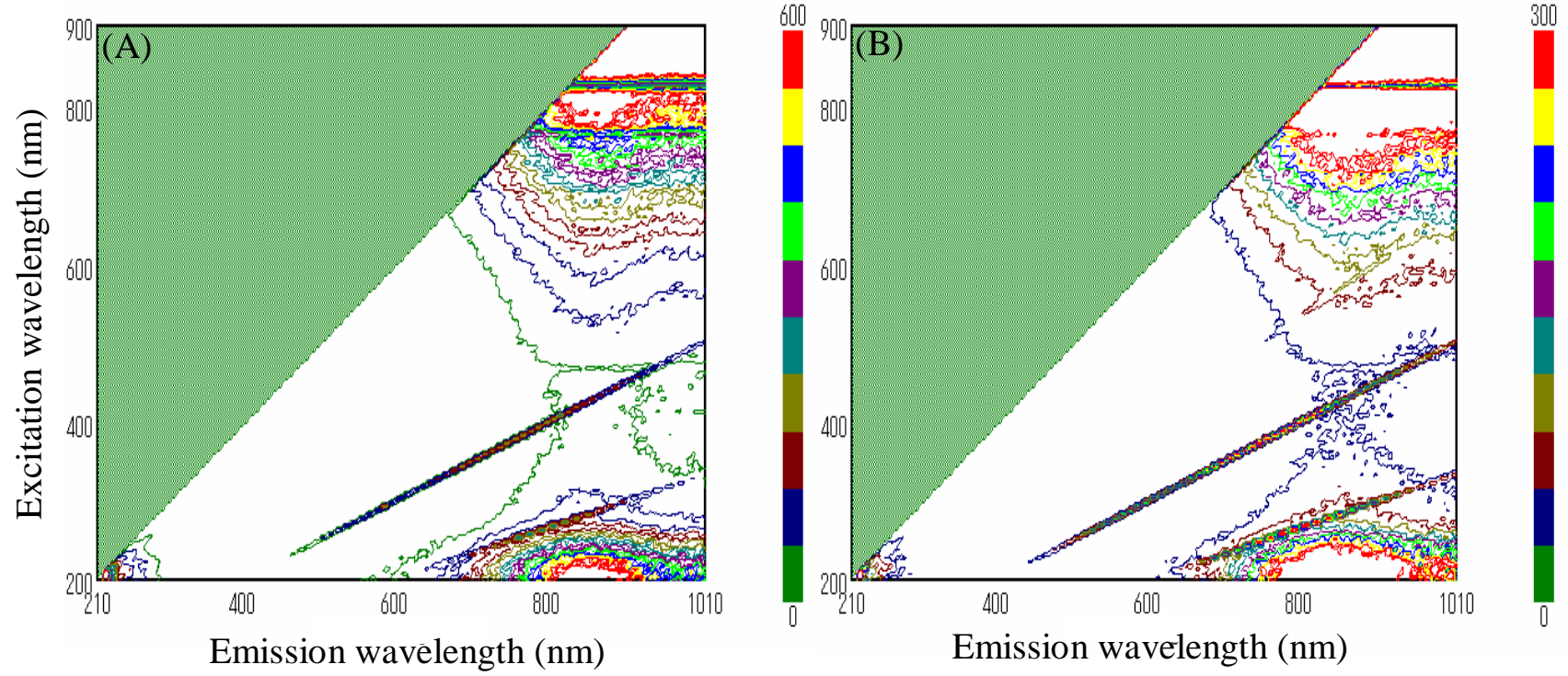


TEM images of (A) AuNRs-SWNTs composite acquired at 300 keV.

Possible impurities

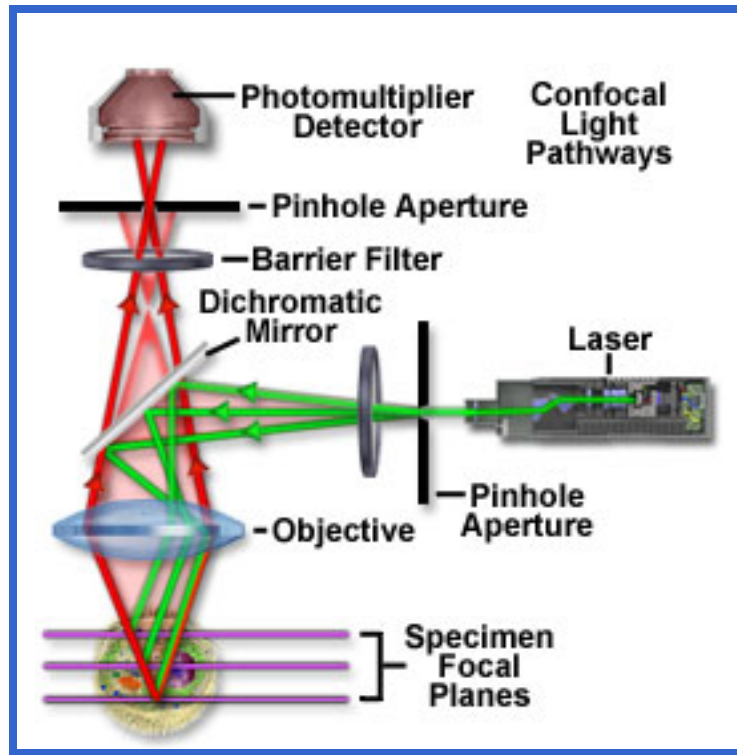


XPS spectra of Au-SWNT composite in the (A) Ni 2p and (B) Fe 2p regions.
ICP - MS

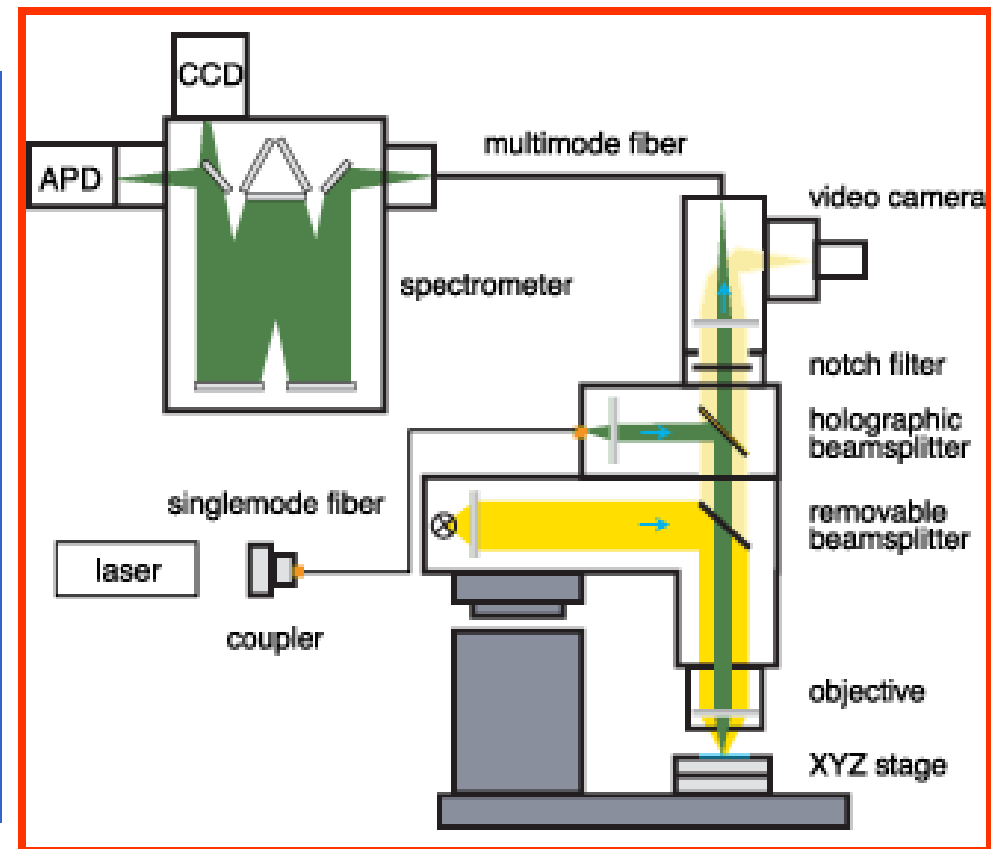


Fluorescence contour plots of (A) supernatant solution and (B) blank water at pH 7.12.

Instrumentation – Confocal Raman



Concept of confocality

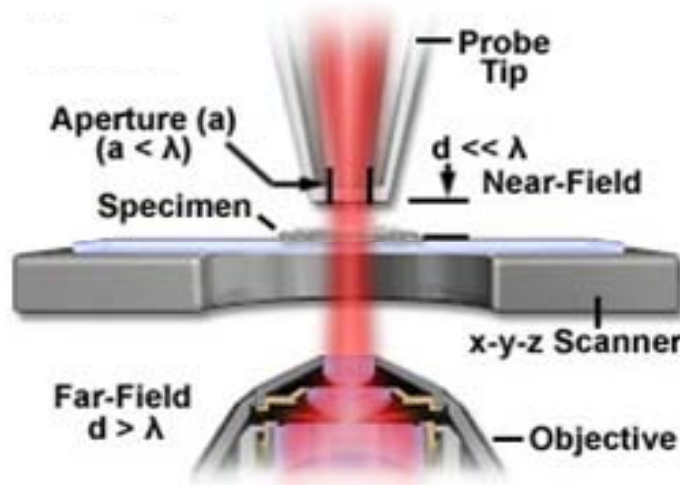


Raman Instrument

Scanning Near-field Optical Microscopy

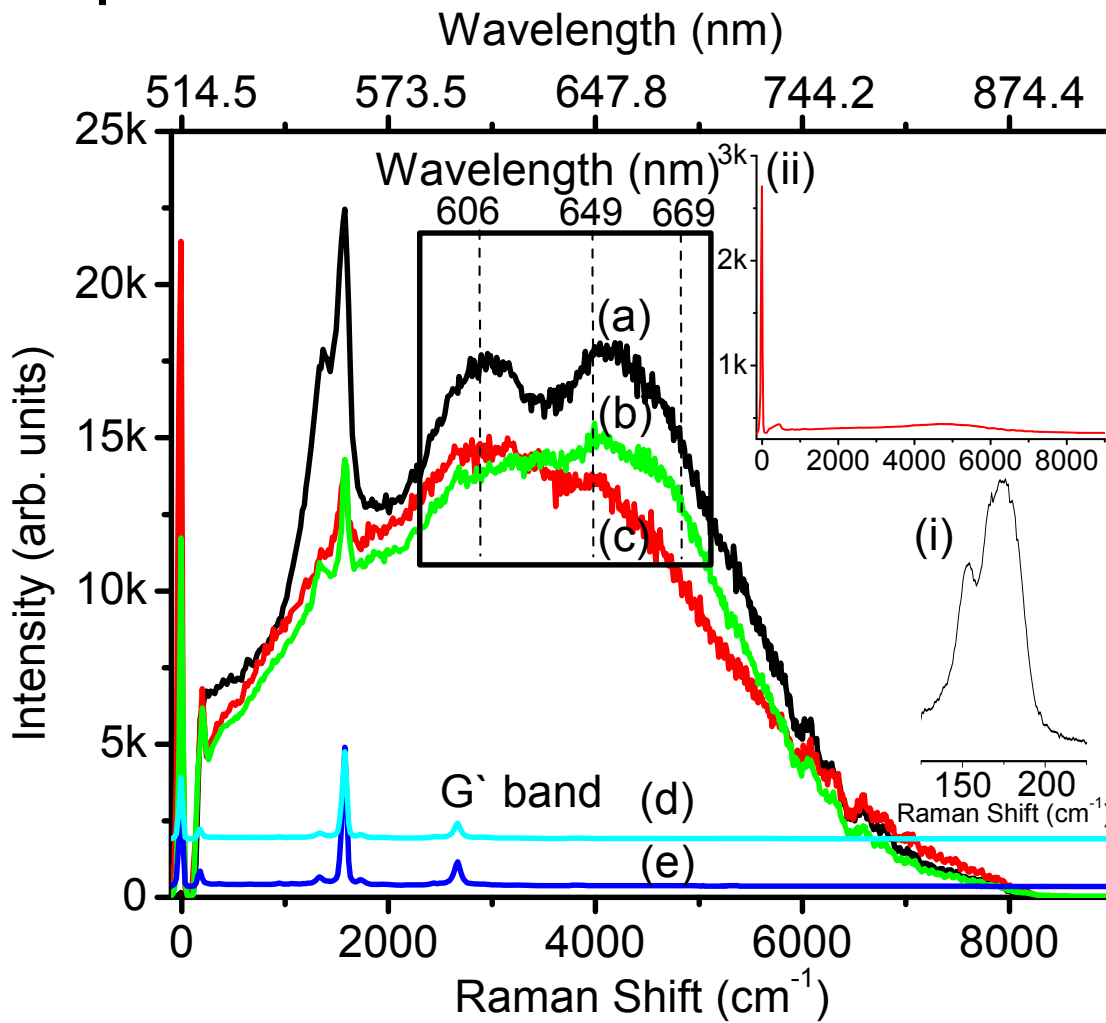
- Resolution is limited by wavelength of light used.
- Near-field microscopy was first proposed by Synge in 1928.

“Resolutions below the diffraction limit can be obtained when the tip-sample distance is smaller than the aperture diameter. In such a case, the aperture diameter controls the resolution and not the wavelength of light used²”



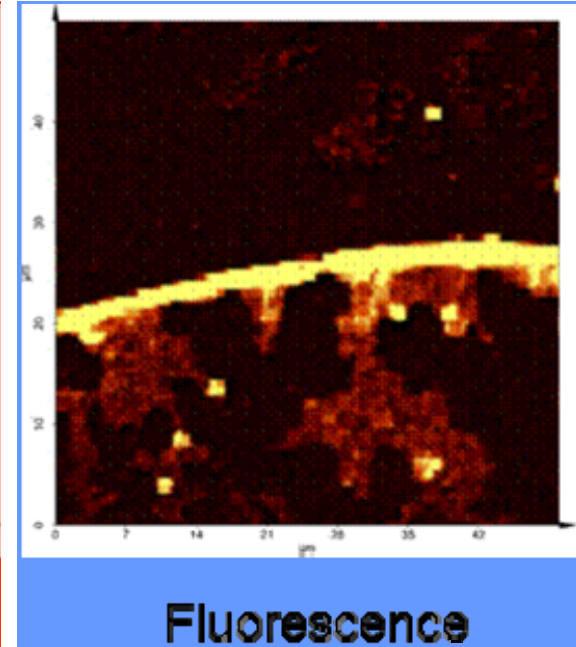
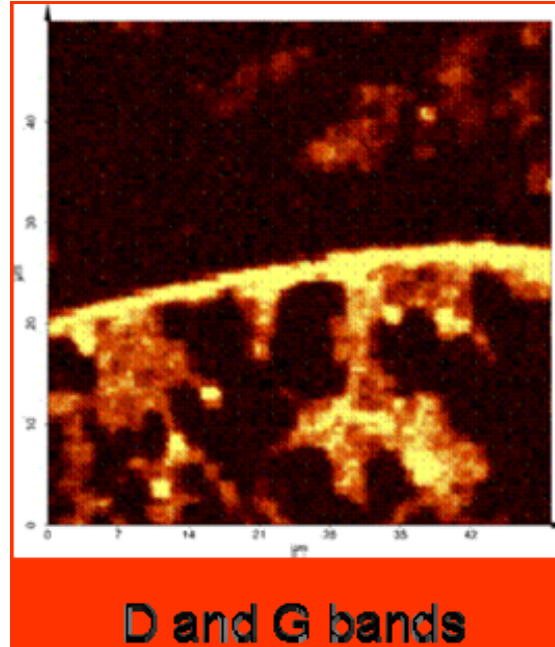
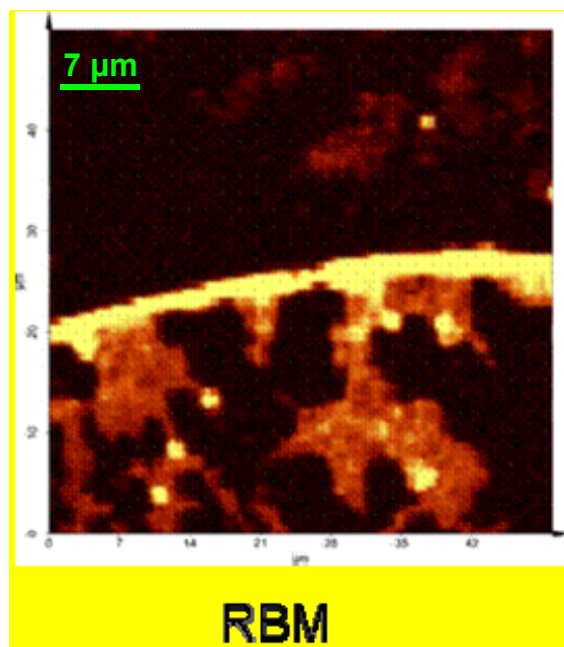
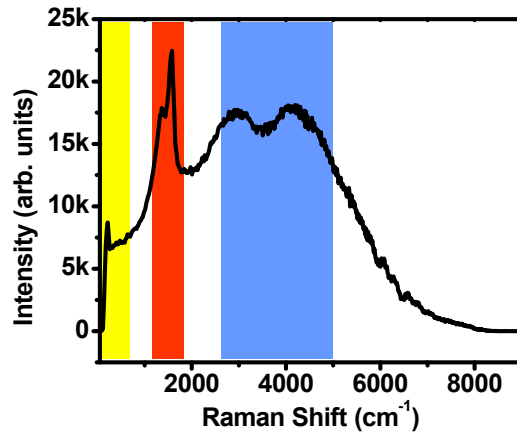
1. www.olympusmicro.com
2. E.H. Synge, *Phil.Mag.* **6**, 356 (1928)

Raman spectra

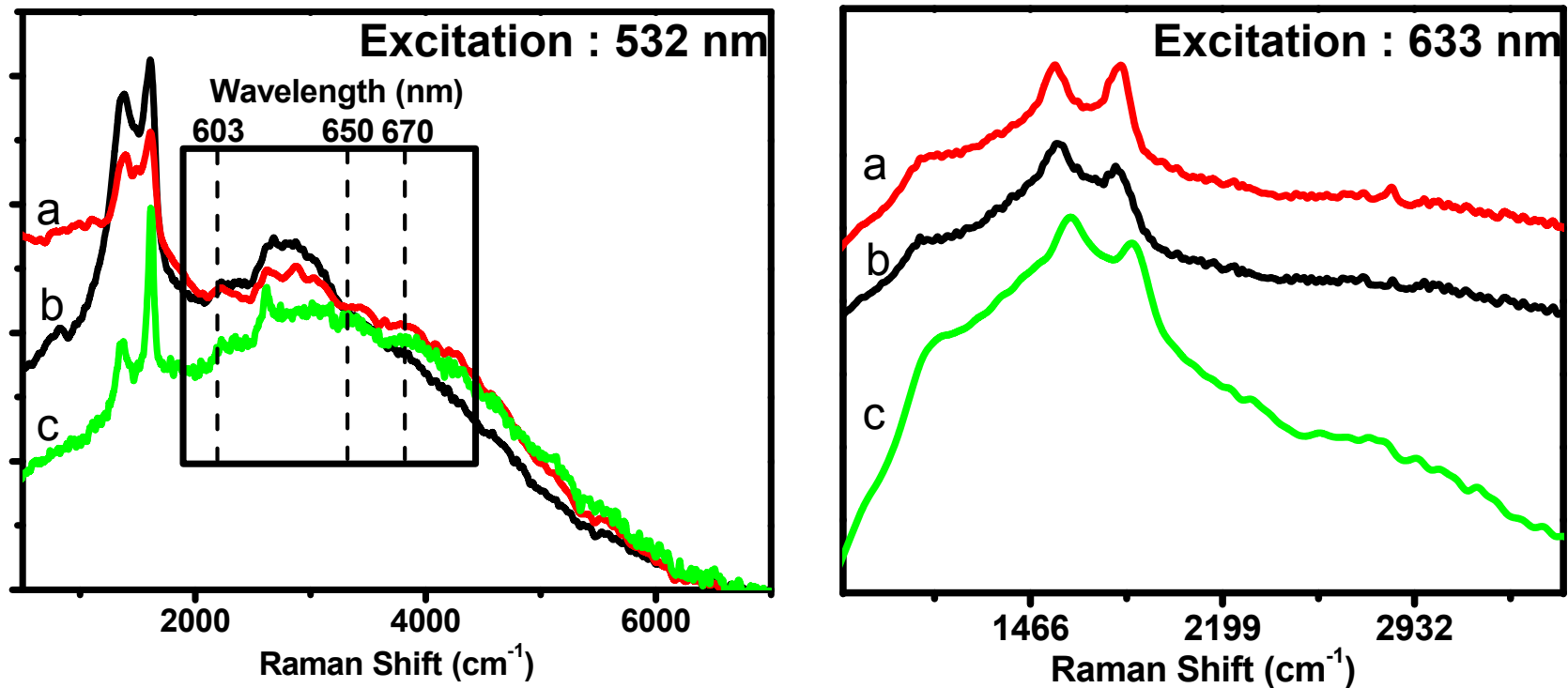


Raman Spectra of (a) Ag-SWNTs composite, (b) Au-SWNTs composite, (c) AuNR-SWNTs composite, (d) pristine SWNTs, (e) Pristine SWNTs treated with trisodium citrate and (f) Au nanorods.

Raman spectral imaging

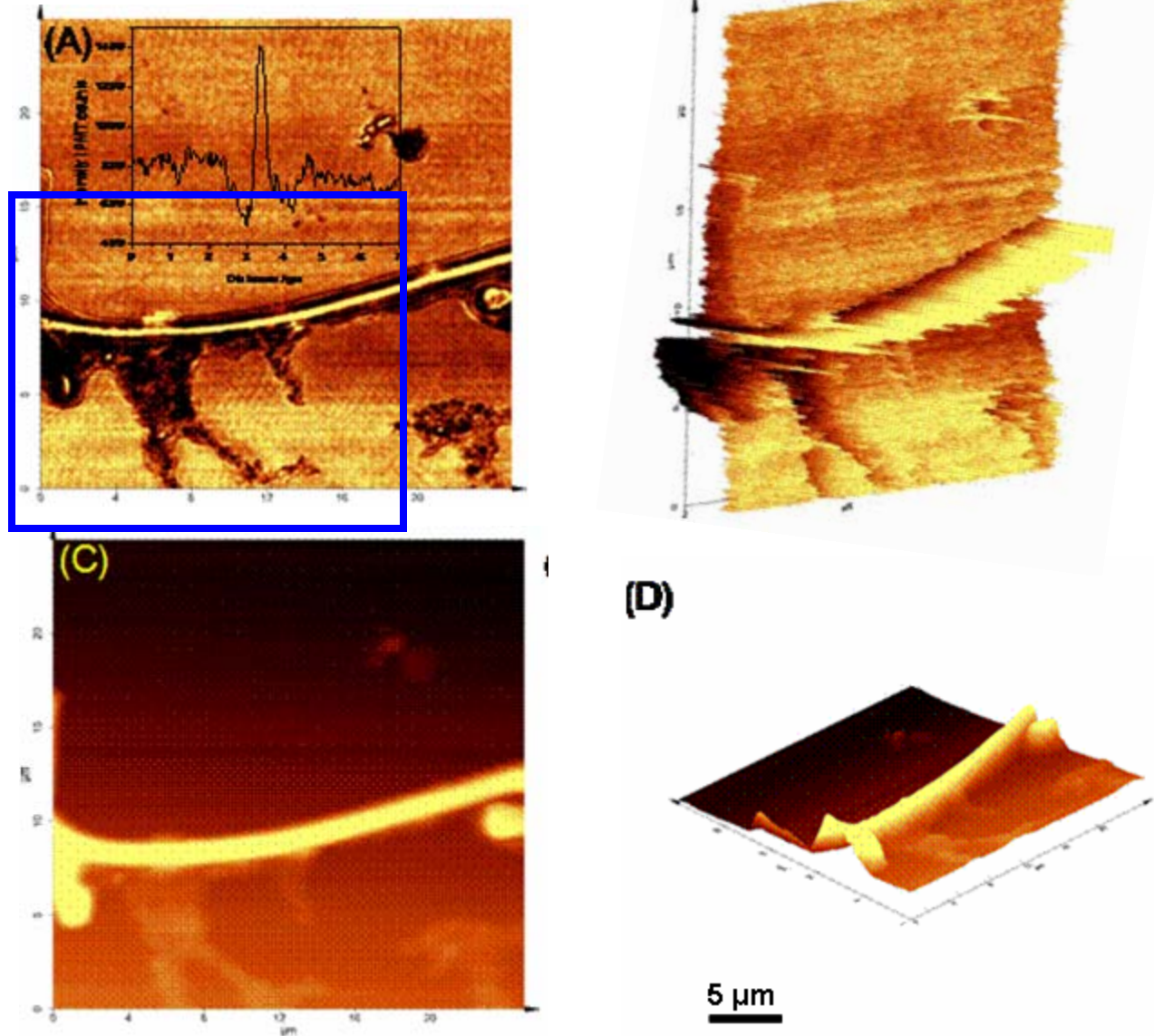


Varying excitation sources

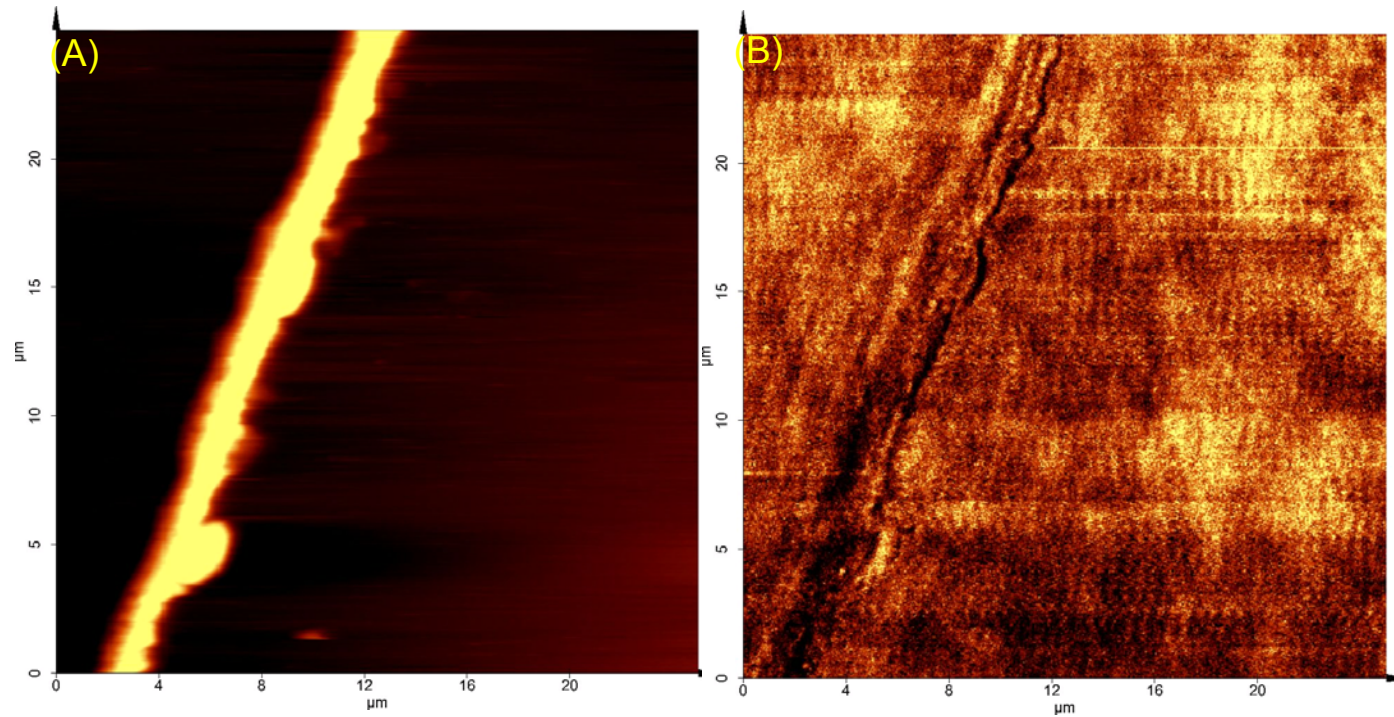


Raman Spectra acquired with (A) 532 nm Nd-YAG and (B) 633 nm He-Ne as excitation sources. Traces (a), (b) and (c) correspond to Ag-SWNTs composite, Au-SWNTs composite and AuNR-SWNTs composite, respectively.

SNOM

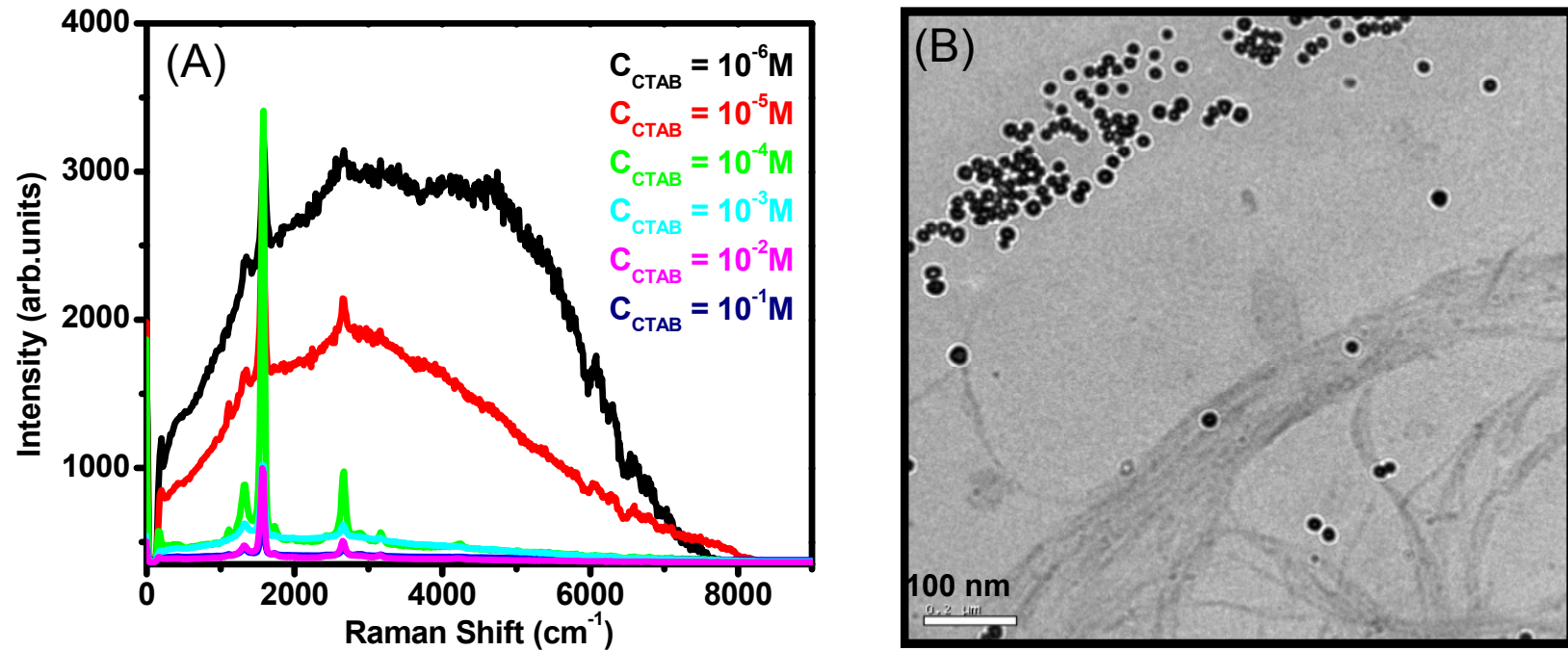


(A) SNOM images of Au-SWNT composite along with the (C) topography. (B) and (D) are their three dimensional representations.

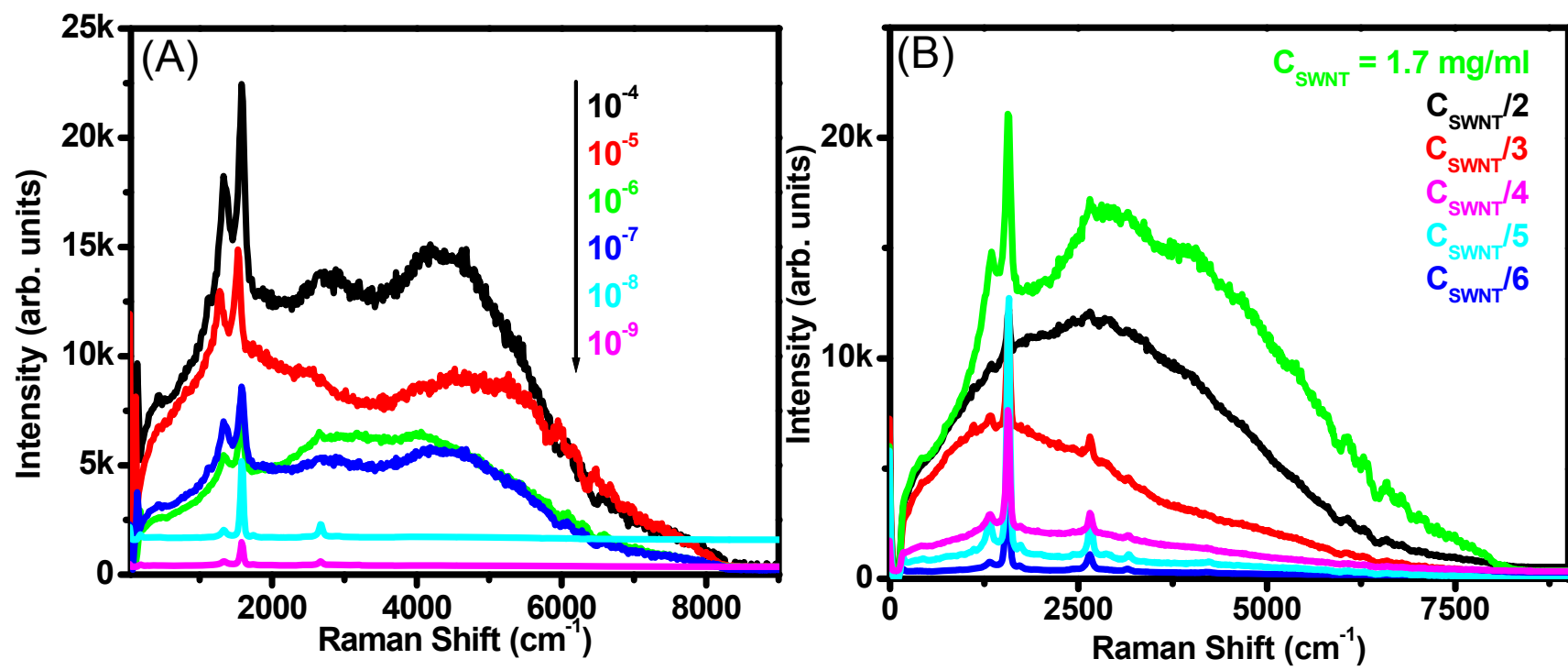


Transmission SNOM images of pristine SWNT based on (A) topography and (B) light intensity.

Supporting experiments

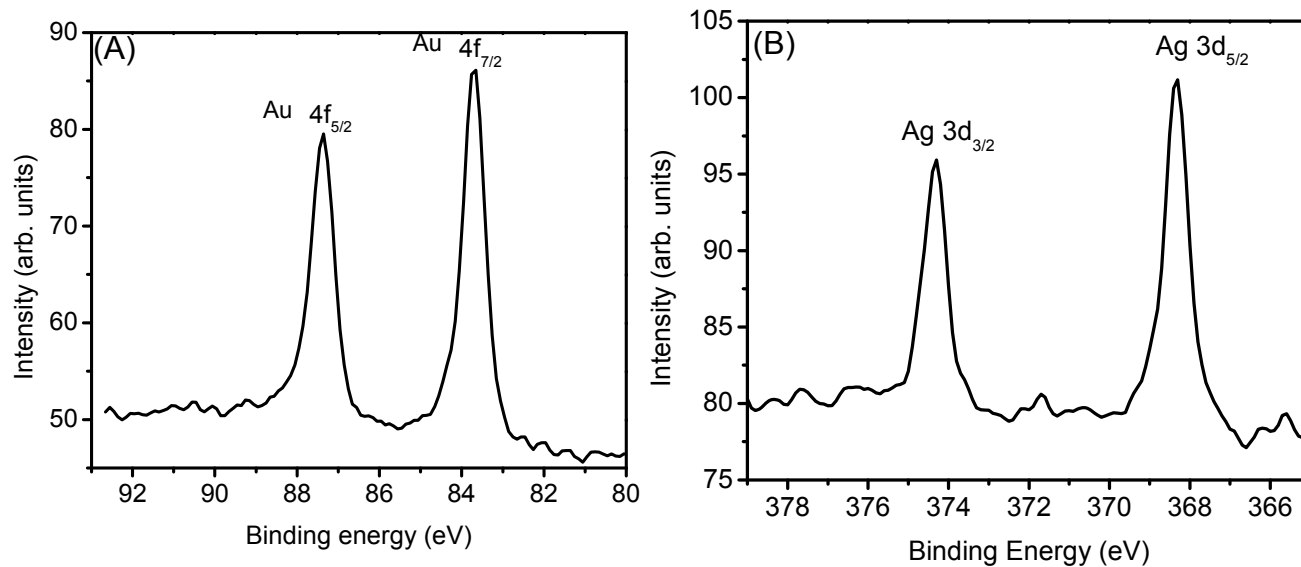


(A) Raman spectra of Ag-SWNT composite measured as a function of CTAB concentration. (B) TEM image of Au-CTAB-SWNT at $C_{\text{CTAB}} = 10^{-4}\text{M}$



Raman spectra of Ag-SWNT composite, measured as a function of (A) concentration of Ag nanoparticles, (B) SWNT concentration.

XPS

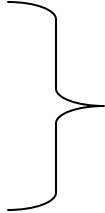


XPS spectra of (A) Au-SWNT and (B) Ag-SWNT composites in the Au 4f and Ag 3d regions, respectively

(n,m) indexing

$\omega_{RBM} = \frac{C_1}{d_t} + C_2$, where C_1 and C_2 are constants

$$d_t = \frac{\sqrt{3}a_{c-c}}{\pi} \sqrt{n^2 + nm + m^2}$$

(n,m)	RBM (cm ⁻¹ , Theoretical)	d_t (nm)	
(10,10)	175	1.37	
(18,0)	168	1.43	
(13,7)	172	1.40	
(17,0)	178	1.35	
(11,9)	175	1.37	
(12,8)	174	1.38	

What we know so far

- ✓ Visible fluorescence from SWNTs is demonstrated.
- ✓ Raman spectral mapping is done to ascertain the origin of fluorescence.
- ✓ SNOM of SWNT structures is done using this fluorescence.

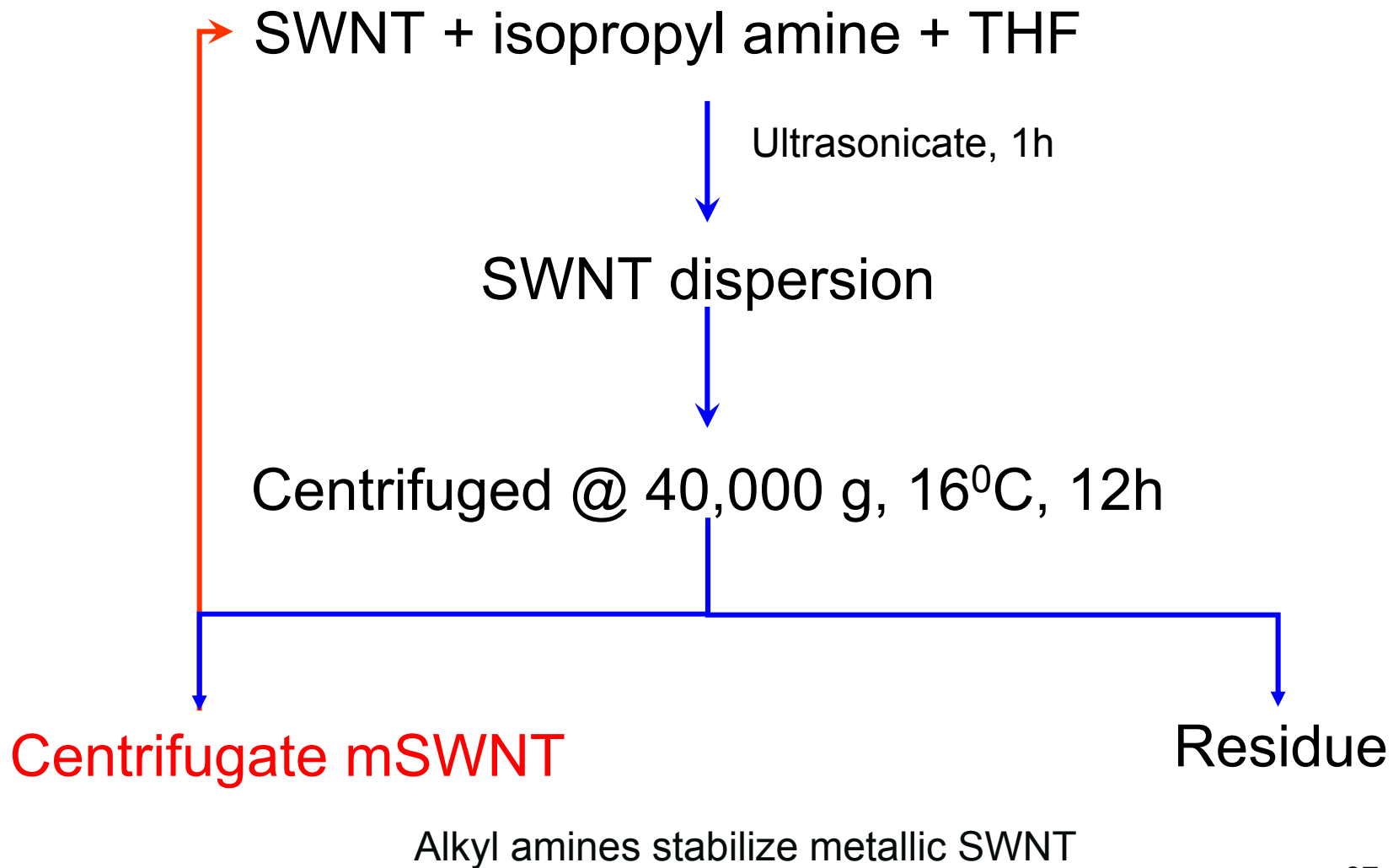
Origin of visible fluorescence

- ⊕ Near-infrared fluorescence in isolated SWNT is known.
- ⊕ This is not observed in bundles and metallic SWNTs.
- ⊕ Metallic SWNTs offer non-radiative decay channels. As metallic SWNTs are present in the bundles, they are not expected to fluoresce.

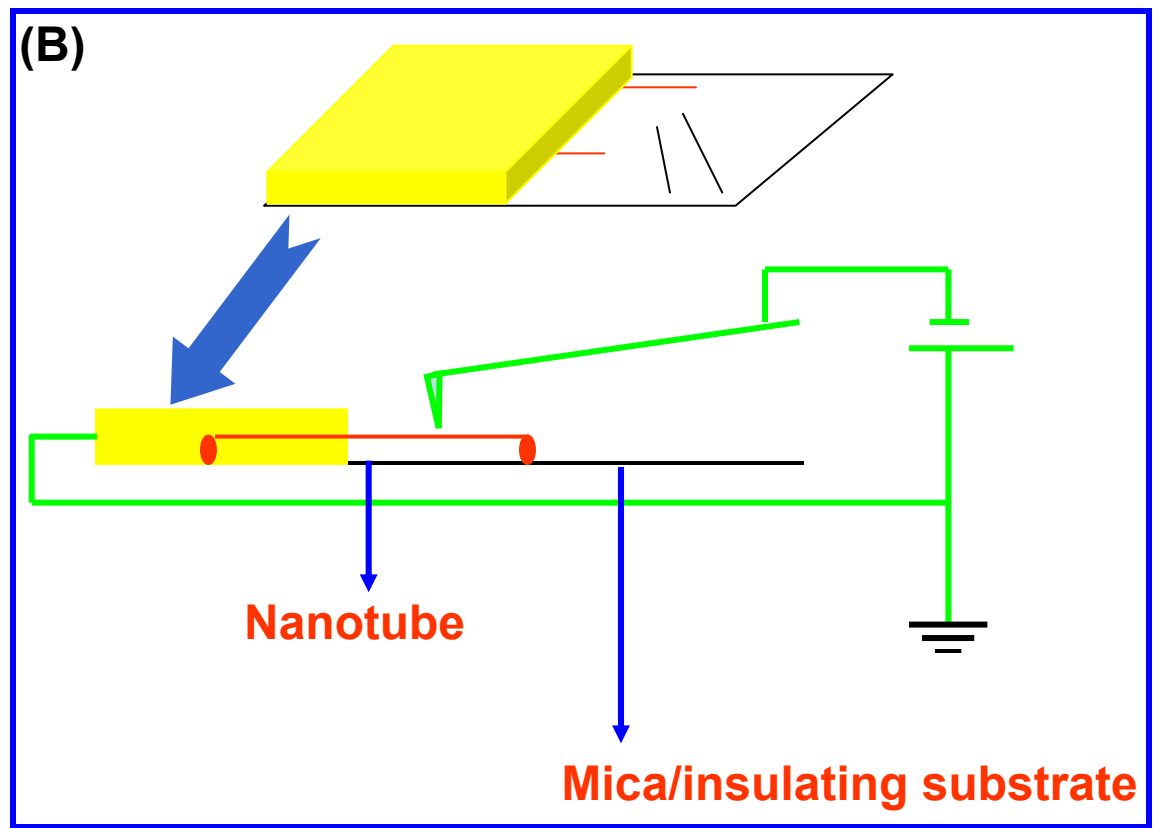
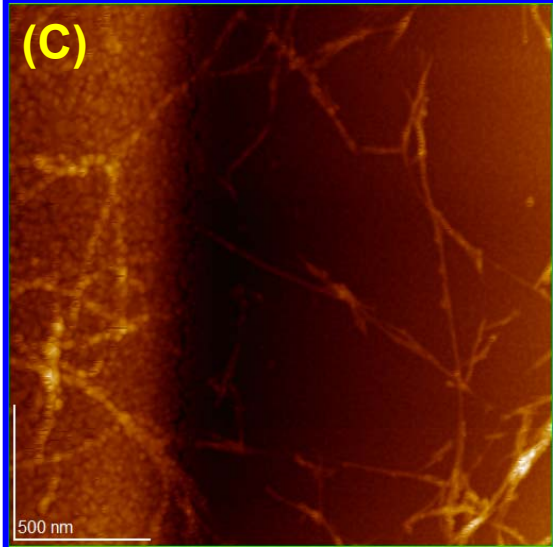
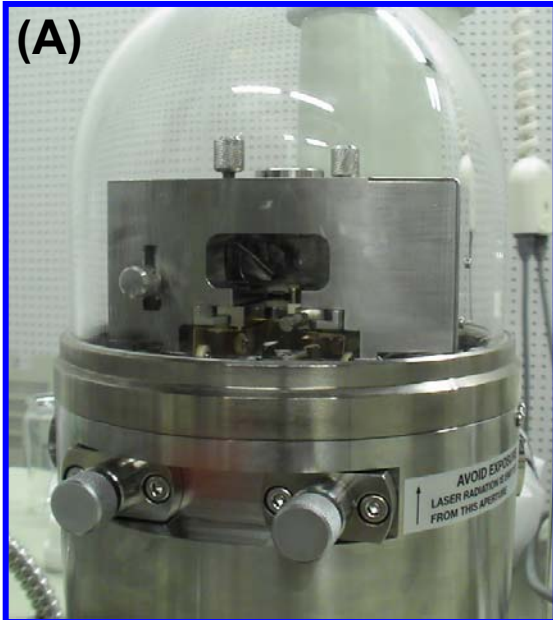
*So what happens to the metallic SWNTs
present in the composite?*

Investigations on mSWNTs

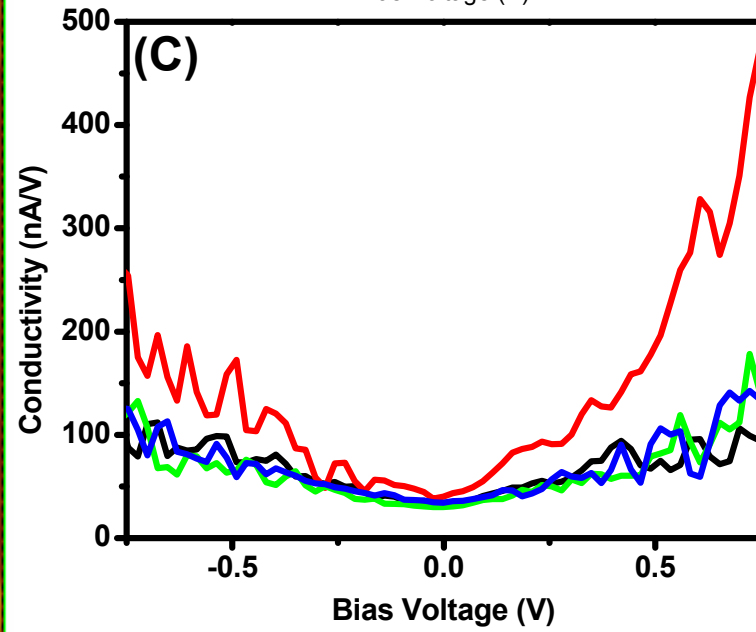
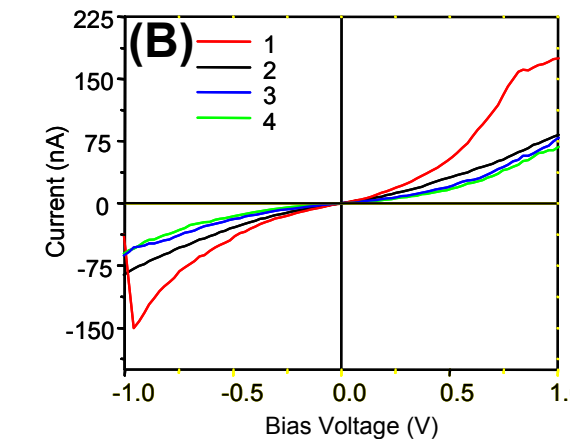
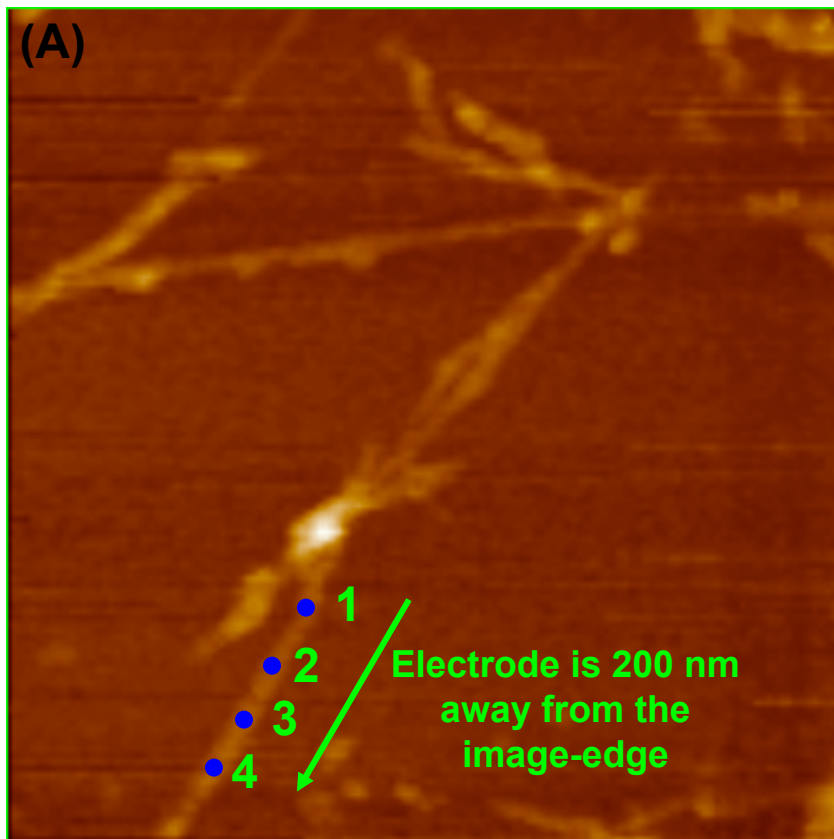
Separation protocol



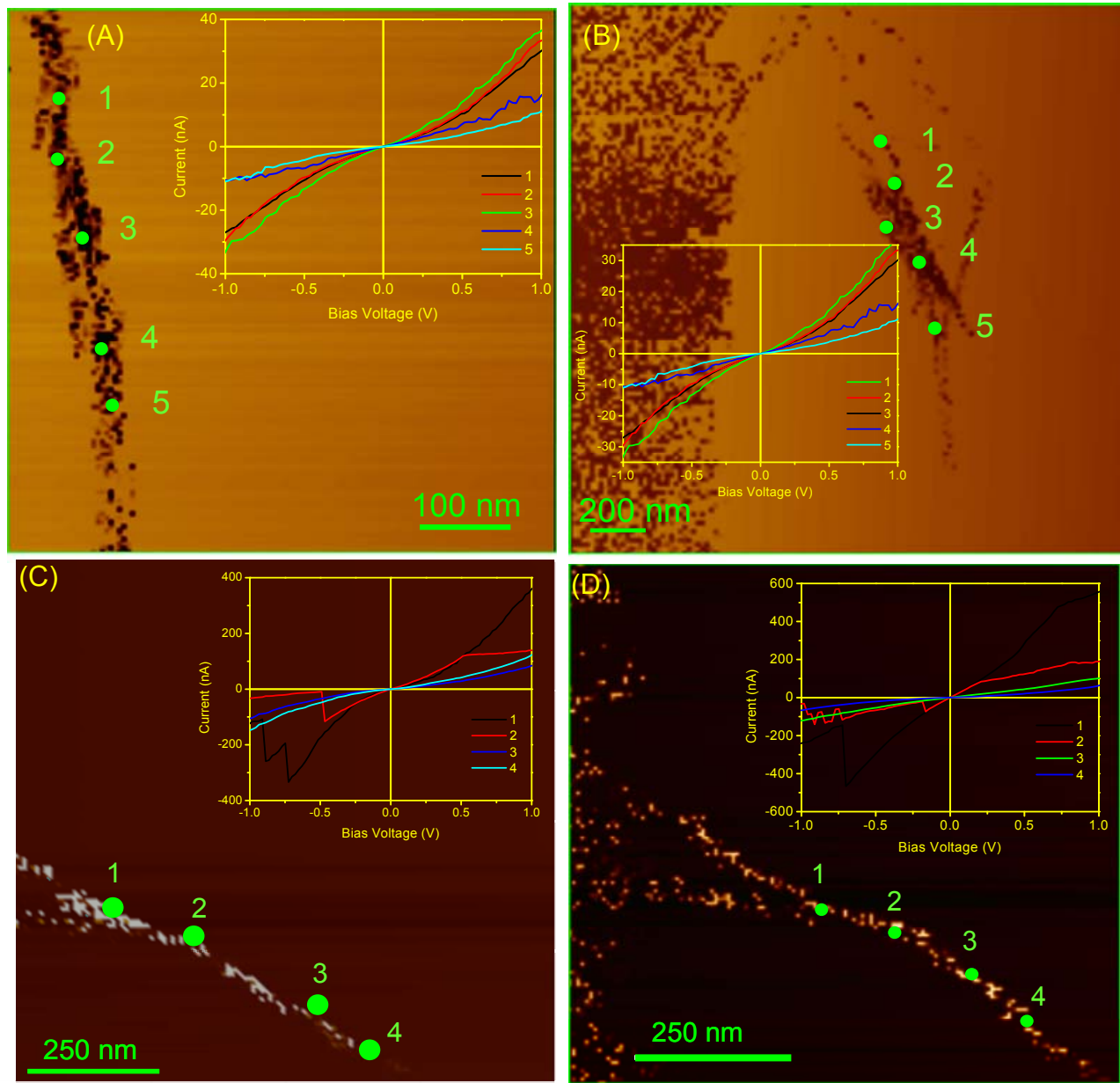
Measurement geometry

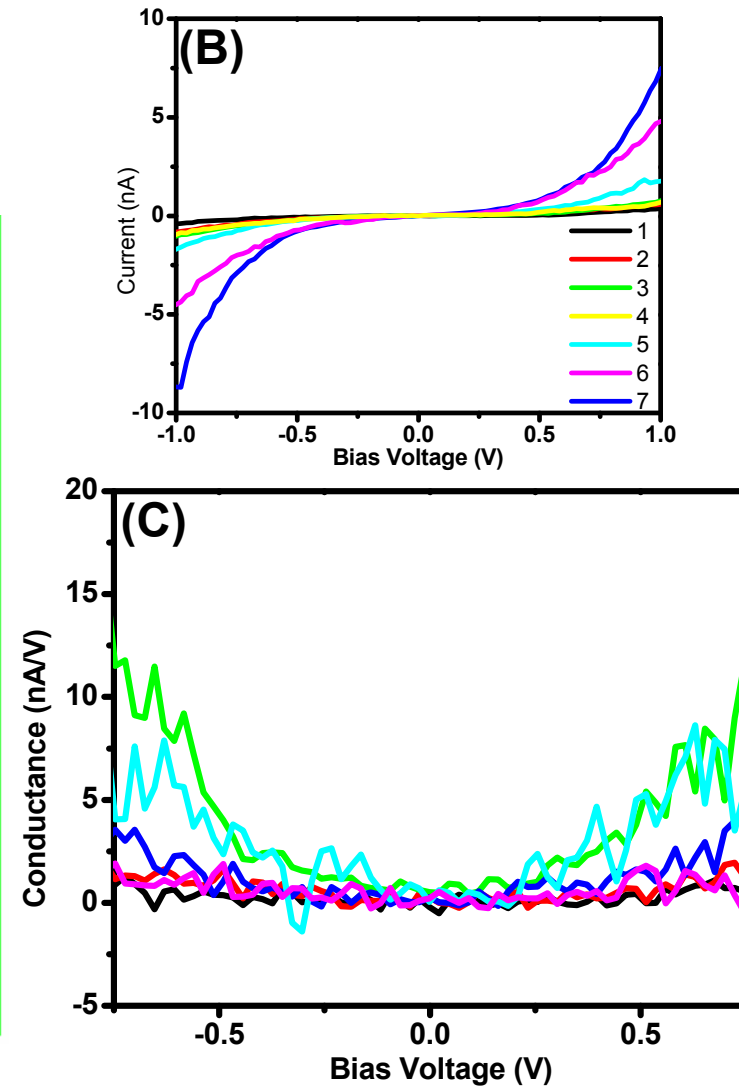
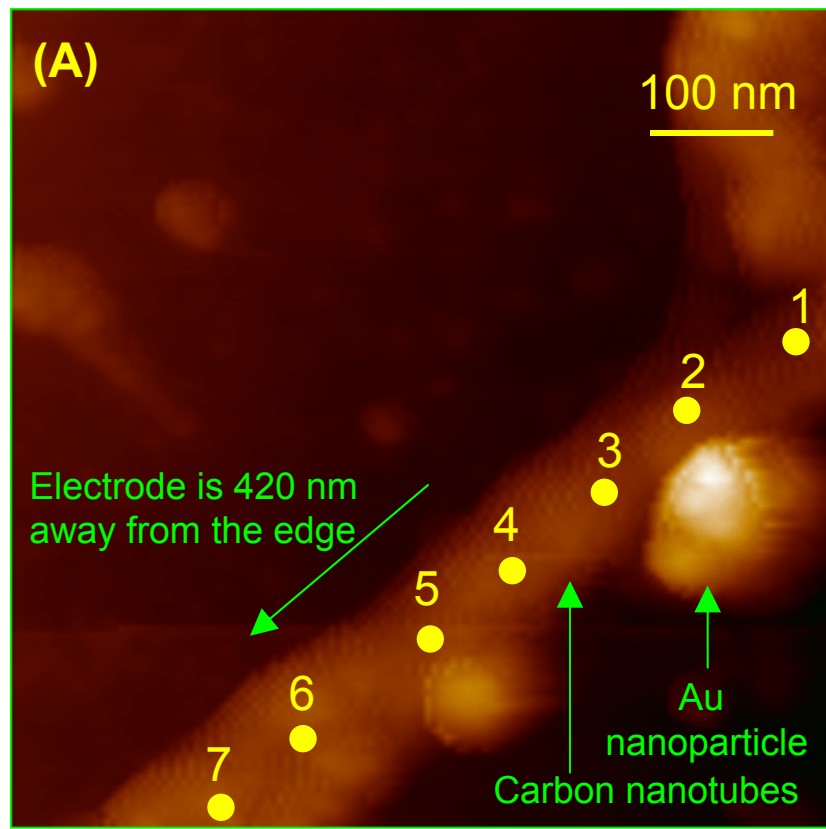


(A) Photograph of the scanning head, (B) schematic of the PCI-AFM measurement and (C) representative AFM image of pristine SWNTs

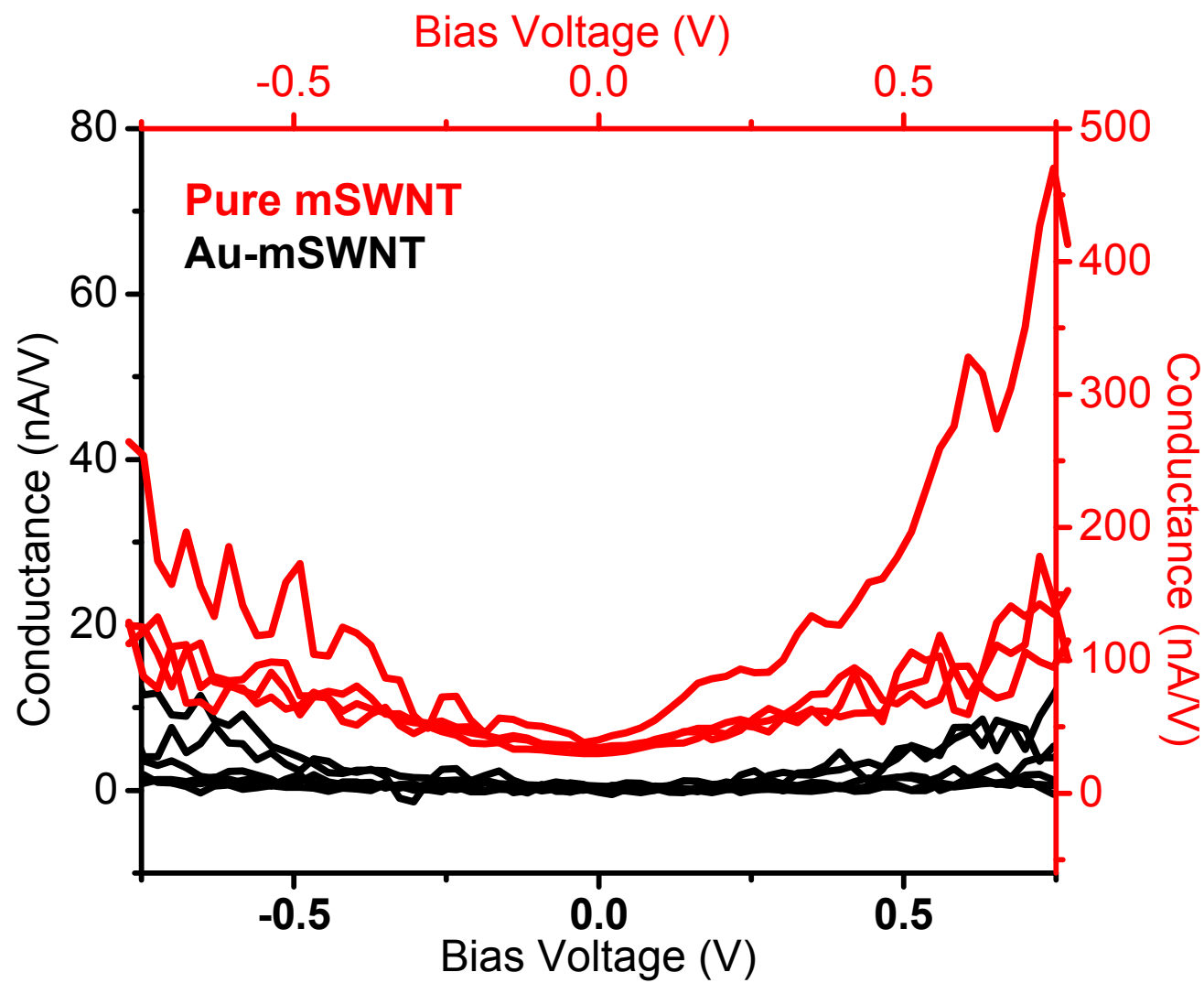


(A) PCI-AFM images of pure mSWNT with (B) I-V curves and (C) plot of conductance versus bias voltage.



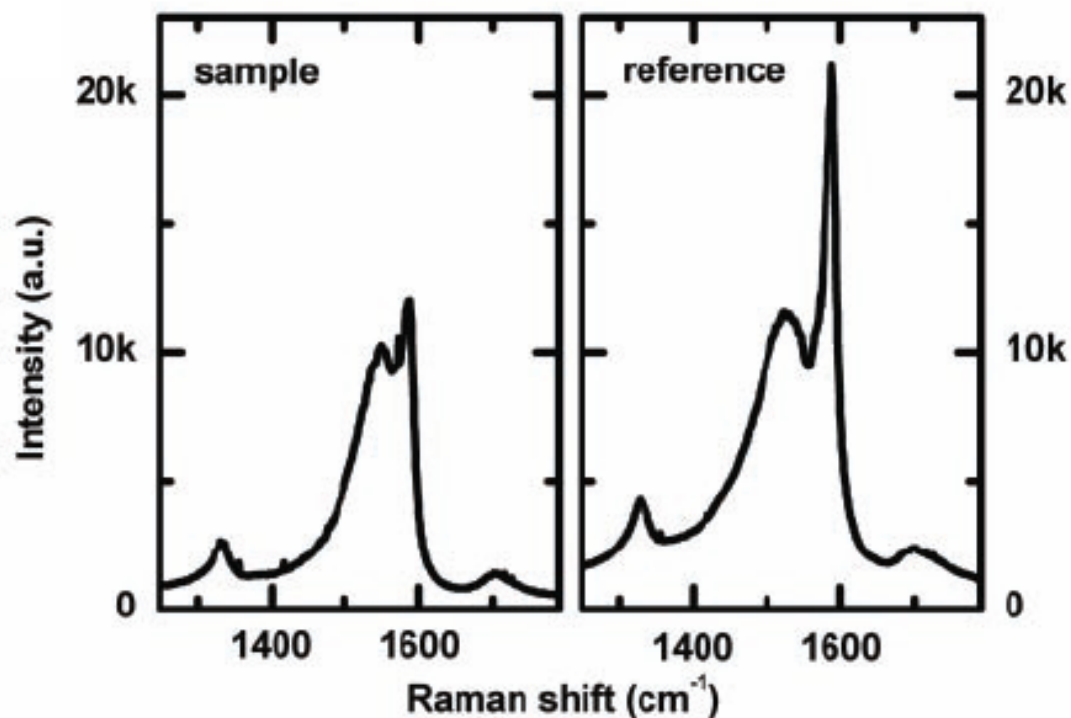


(A) PCI-AFM image of Au-mSWNT with (B) the corresponding I-V curves and (C) Plot of conductance versus bias voltage.



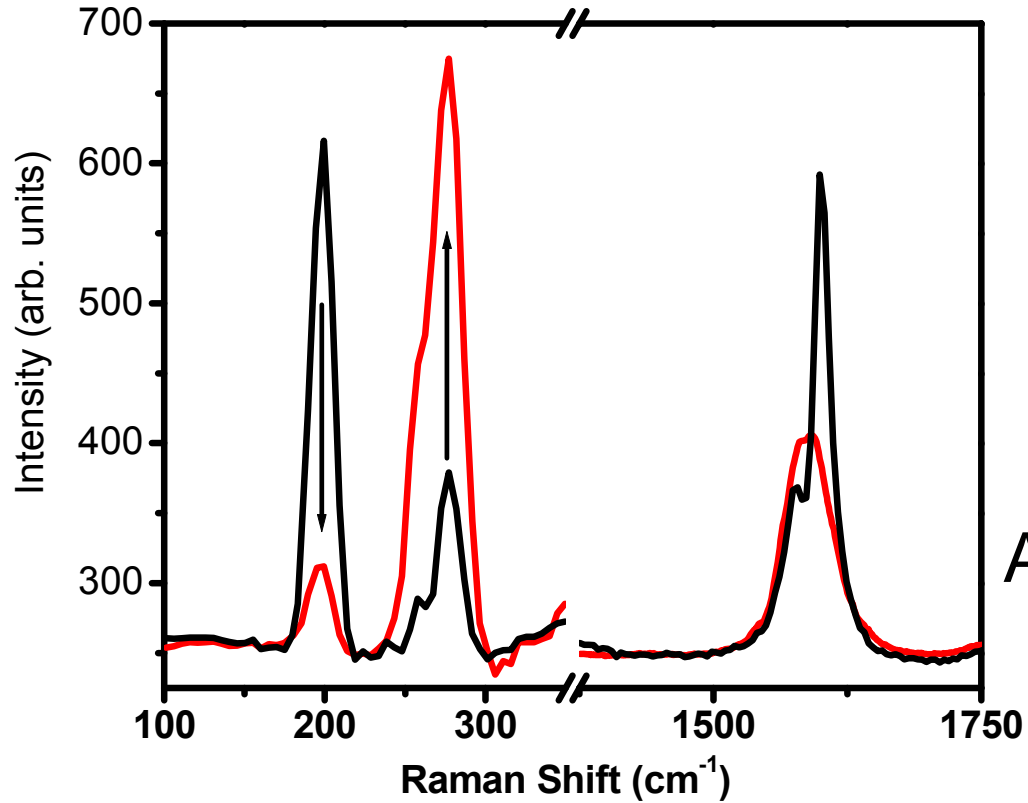
Comparison of conductance versus bias voltage for **pure mSWNT** and **Au-mSWNT** composite

G-band line shapes of metallic and semiconducting SWNT



Changes observed in G-band for metallic (left) and pristine (right) SWNT

➤ Confocal Raman investigations

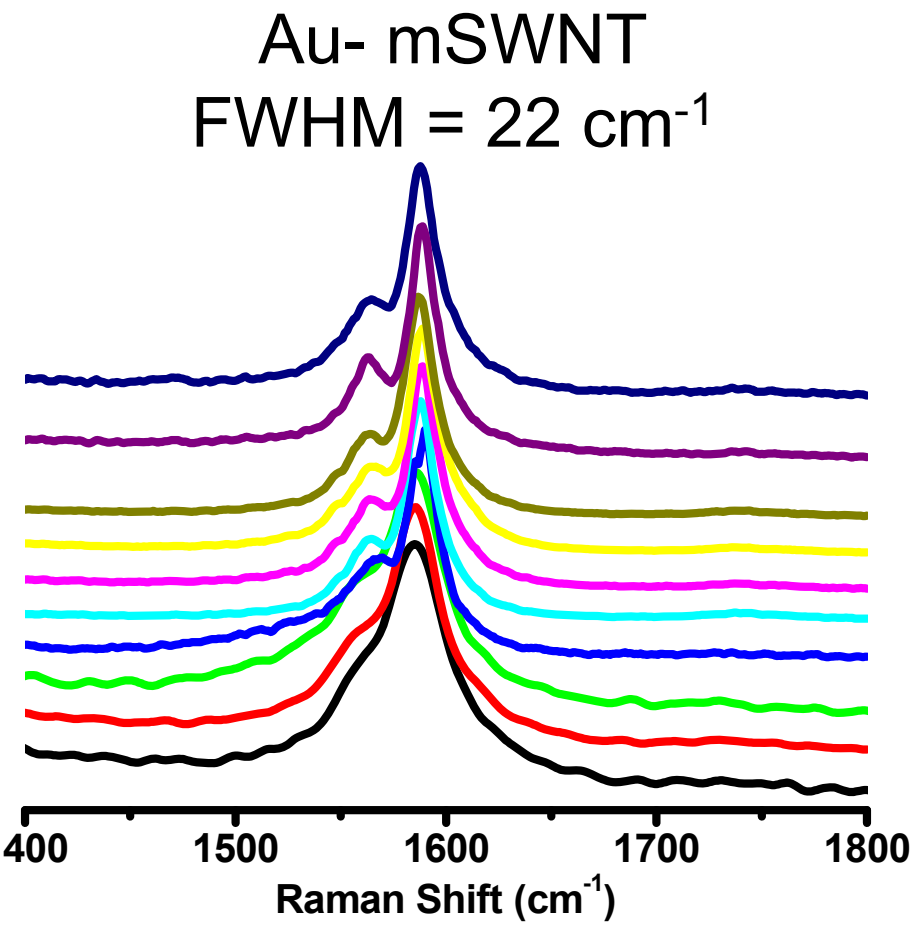
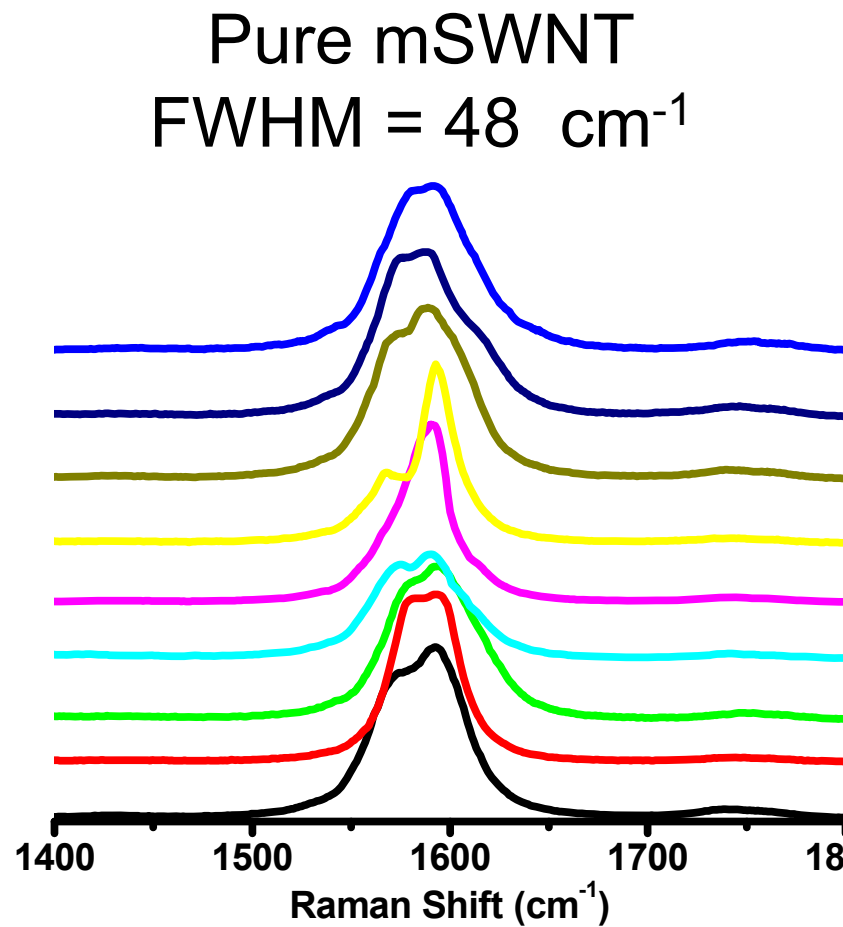


$$A_s/A_m = 65.0$$
$$A_s/A_m = 0.14$$

Extraction efficiency

$$A_s/(A_s + A_m)^* 100 = 88\%$$

Raman spectra in RBM and G-band regions of pristine SWNT (black) and **extracted mSWNT (red)**.



Comparison of G-band of pure mSWNT and Au-mSWNT

What we know:

Metallicity of SWNT is destroyed by interaction with nanoparticles.

PCI-AFM and confocal Raman confirm this M-S transition.

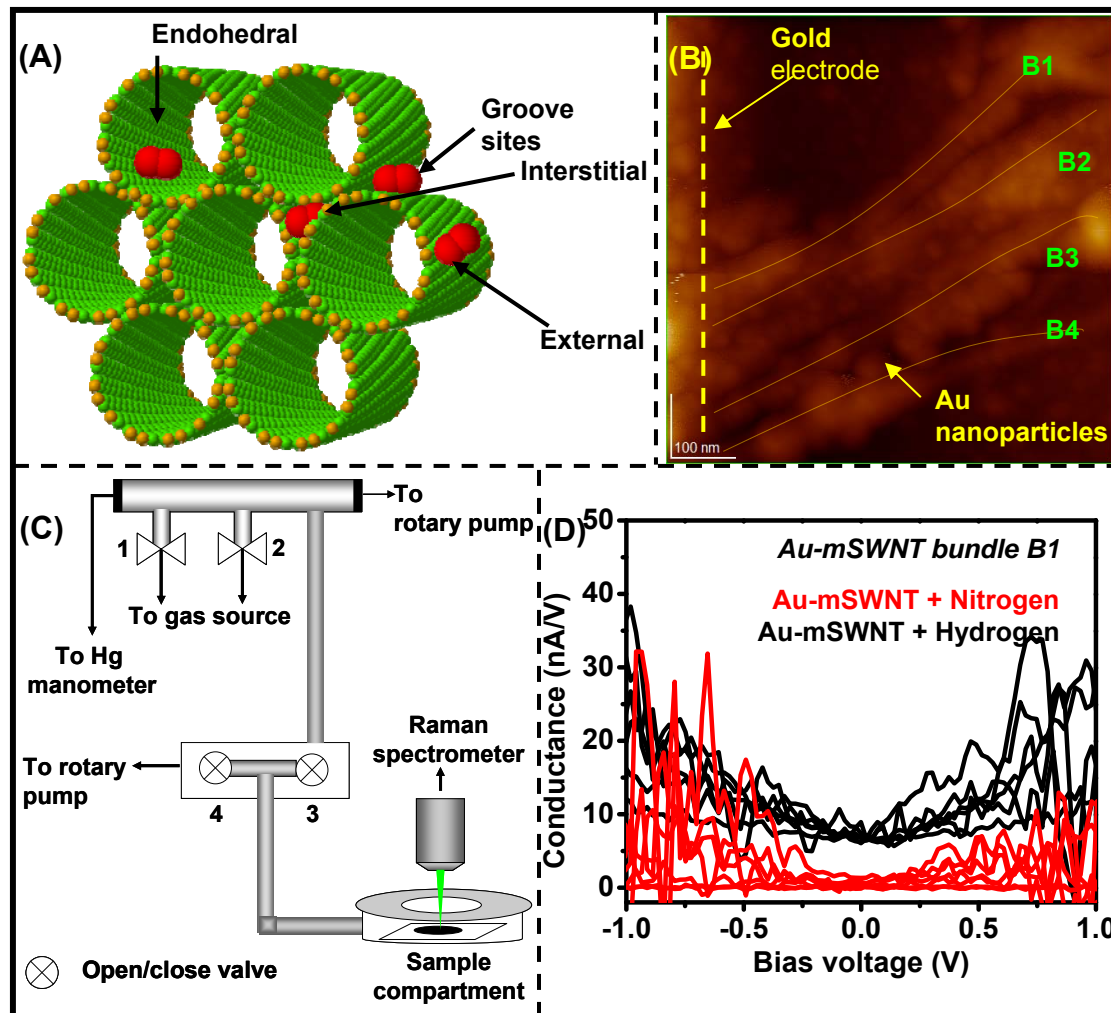
mSWNT fluoresce when their metallicity is destroyed.

M-S transition has far reaching implication in nanoelectronics and design of nanodevices.

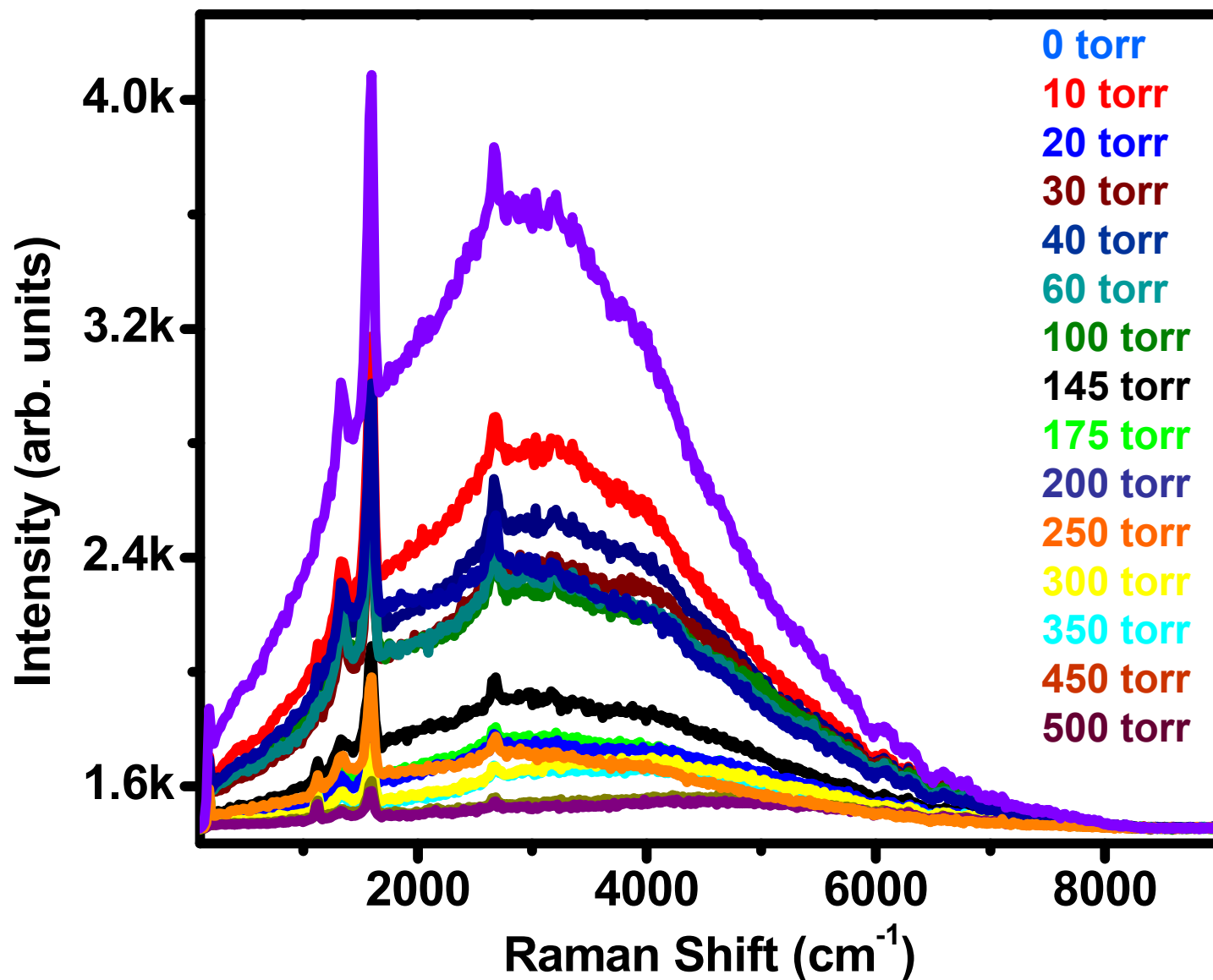
C. Subramaniam *et al.* Phys. Rev. Lett. (2007)

C. Subramaniam and T. Pradeep Patent applications 2006, 2007

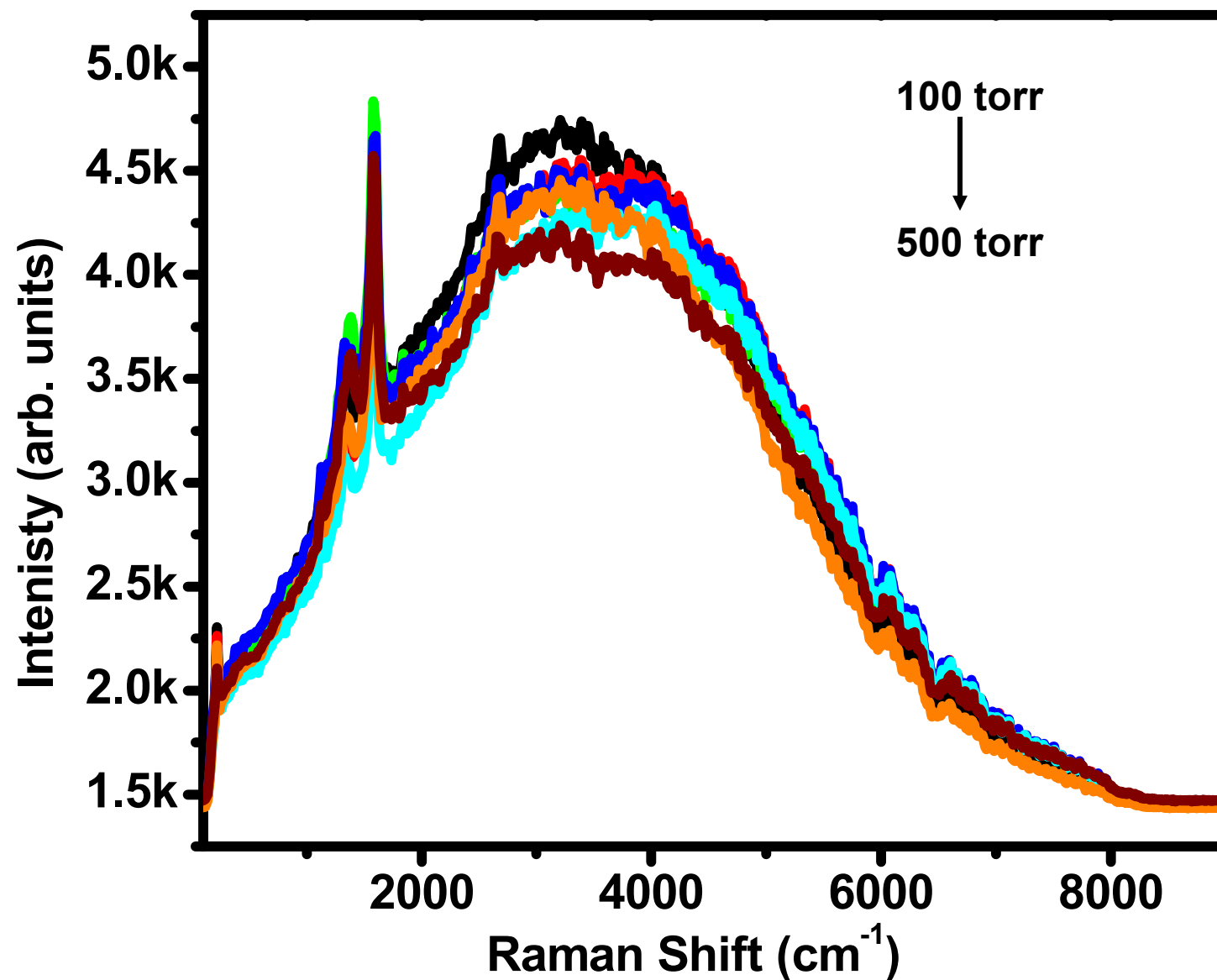
Nanotube gas sensors using fluorescence



(A) Schematic representation of a SWNT bundle with the adsorption sites indicated. (B) Topographic image of Au-mSWNT composite. Several points on various bundles marked B1 to B4 have been analyzed through PCI-AFM. The gold electrode and the bundles have been marked with guide lines. (C) Schematic representation of the microRaman setup used for gas-exposure studies. (D) Plot of conductance versus bias voltage constructed from various points of the bundle labeled B1 in Figure 1B, under an atmosphere of nitrogen (red traces) and hydrogen (black traces). 48

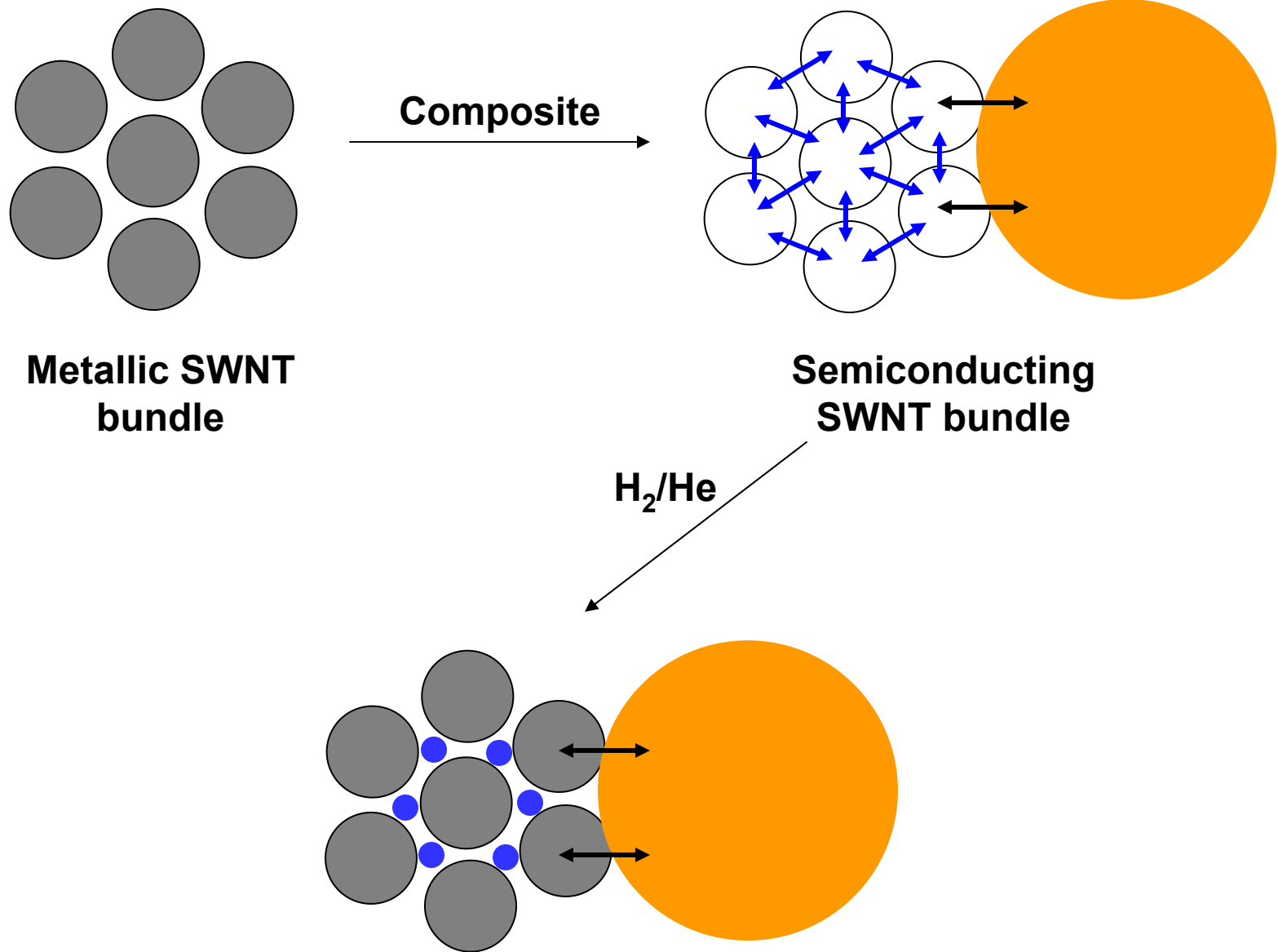


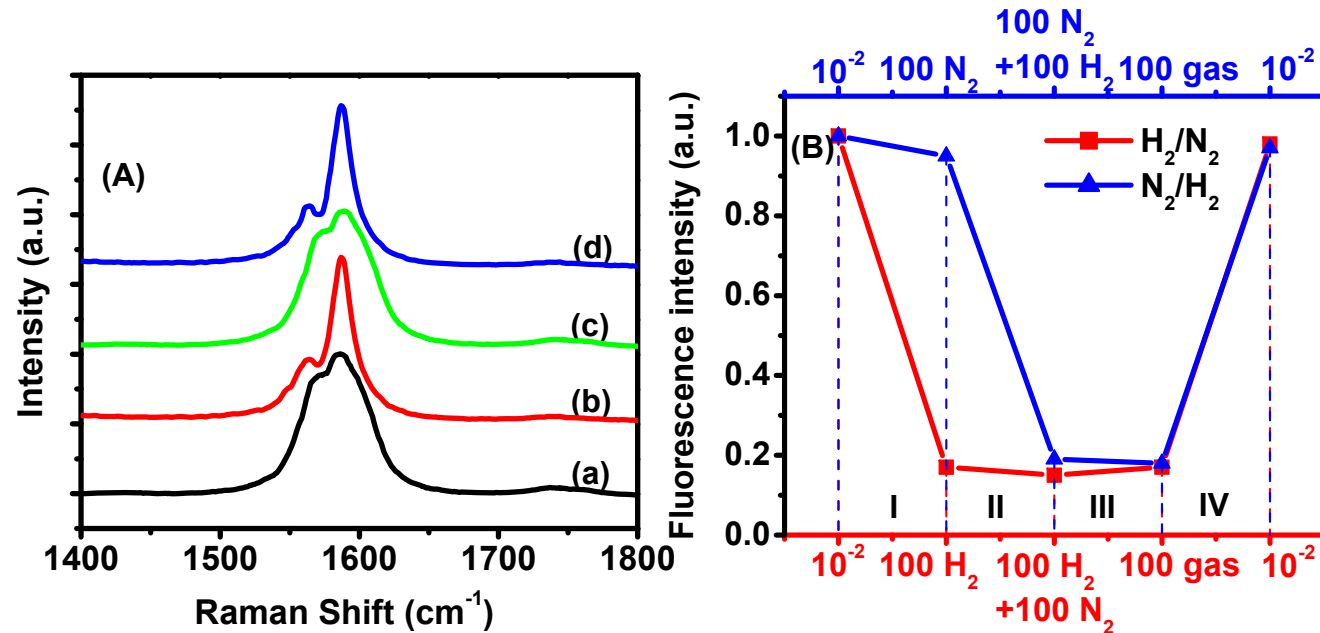
Au-SWNTs exposed to H_2 gas at various partial pressures.



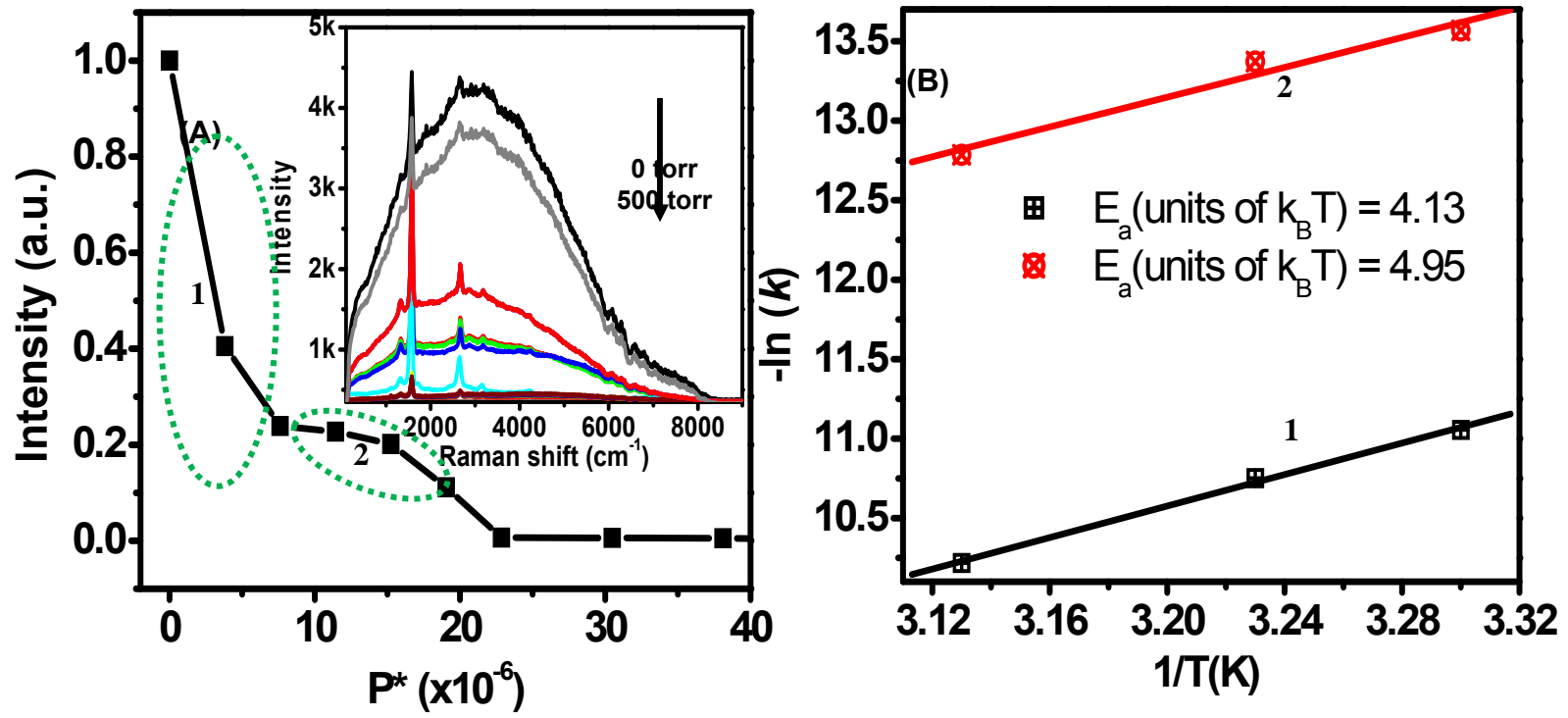
Au-SWNTs exposed to N_2 gas at various partial pressures.

Suggested mechanism

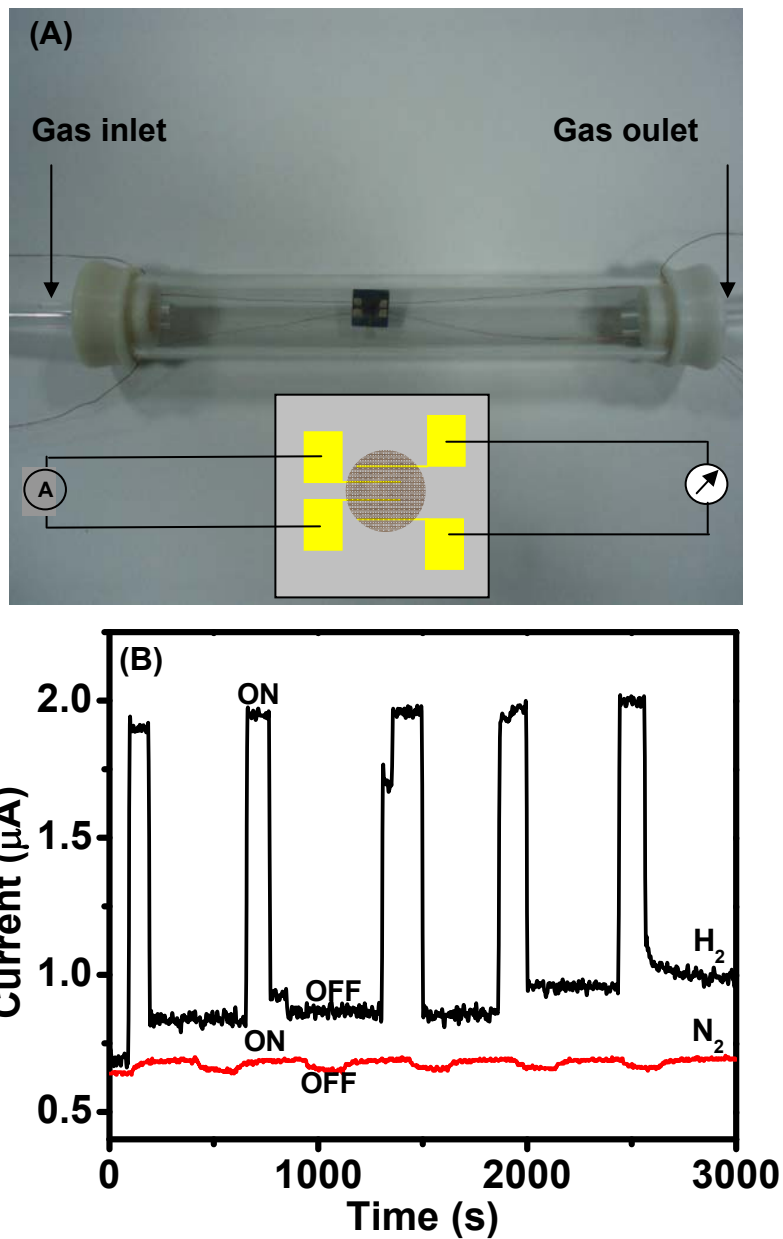




(A) Raman spectra of (a) purified *m*SWNTs, (b) Au-*m*SWNT composite, (c) Au-*m*SWNT upon exposure to 500 torr H₂ and (d) Au-*m*SWNT composite after pumping out H₂ exposed in (c). Spectra (a) to (d) are recorded at the same point on the composite sample. (B) Variation of fluorescence intensity upon exposing mixture of gases. Regions A to D are explained in the text. Pressures are in torr.



(A) Plot of normalised fluorescence intensity versus P^* for Au-mSWNT. The corresponding spectral variation with increasing pressure of H₂ for some of the pressures is shown as inset. Grey trace shows the recovery spectrum upon immediate pumping. Complete recovery is obtained upon pumping for 15 minutes. The two regions having different slopes are circled in green and marked as 1 (interstitial adsorption) and 2 (external adsorption). (B) Arrhenius plot of $-\ln k$ at different temperatures versus $1/T$. Interstitial adsorption (1, black), groove and external adsorption (2, red) are indicated.



(A) Photograph of the device setup with a cartoon representation of the microelectrode. The shaded circle in the cartoon is used to represent the sample with the yellow regions representing the gold electrode. (B) A plot of variation of current for a bias voltage of 5 V for Au-mSWNT composite in presence of H_2 (500 torr, black line) and N_2 (500 torr, red line). The ON and OFF states pertain to the presence and absence of gases, respectively. While the current for the ON state is constant, that due to the OFF state increases slowly with increase in cycles as hydrogen exposed during the previous cycle is not removed completely, consistent with the fluorescence data (Fig. 3A inset). Current measurements appear to be sensitive to tiny quantities of adsorbed gases.

Summary and conclusions

Metal nanoparticles upon interaction, destroy the metallicity of carbon nanotubes.

This makes SWNTs emit light in the visible region of the spectrum.

Visible light emission is sensitive to gases which adsorb in the interstitial sites of SWNT bundles.

A device based on this property has been demonstrated.

C. Subramaniam and T. Pradeep Patent applications 2008

C. Subramaniam et al. Submitted



Nano Initiative of the DST





Swarnajayanti project, DST



IIT Madras

Thank you all